AFCRL 65-155

FEBRUARY, 1965

DIVISION OF ENGINEERING RESEARCH AND DEVELOPMENT

DEPARTMENT OF ELECTRICAL ENGINEERING

Love Wave Diffraction In A Variable Thickness Surface Layer

by
DAVID JOSEPH DEFANTI
and
JOHN E. SPENCE

Contract No. AF19 (628) - 319
Project No. 8652
Task No. 865203
Scientific Report No. 5

Prepared
for
AIR FORCE CAMBRIDGE RESEARCH LABORATORIES
OFFICE OF AEROSPACE RESEARCH
UNITED STATES AIR FORCE
BEDFORD, MASSACHUSETTS

WORK SPONSORED BY ADVANCED RESEARCH PROJECT AGENCY
PROJECT VELA - UNIFORM
ARPA Order No. 180 - 62 and 292 - 62

Project Code No. $\frac{8100}{3810}$ Task 2

UNIVERSITY OF RHODE ISLAND
KINGSTON, RHODE ISLAND

NOTICES

The following information shall be displayed inside the front cover of all reports except those containing top secret material:

> Requests for additional copies by agencies of the Department of Defense, their contractors, or other government agencies should be directed to:
>
> Defense Documentation Center (DDC)
> Cameron Station
> Alexandria, Virginia 22314
>
> Department of Defense contractors must be established for DDC services or have their "need-to-know" certified by the cognizant military agency of their project or contract.

Unclassified reports, OTHER THAN REPRINTS OF JOURNAL ARTICLES USED AS SCIENTIFIC OR FINAL REPORTS shall display the following additional information under the above notice:

All other persons and organizations should apply to the:

Clearinghouse for Federal Scientific
and Technical Information (CFSTI)
Sills Building
5285 Port Royal Road
Springfield, Virginia 22151

ABSTRACT

Consideration is given to a mathematical analysis of a special case of seismic wave phenomena. In particular, the mixed boundary value problem of Love wave propagation in a solid layer over a solid half-space is investigated where the layer undergoes an abrupt change in thickness. Both the layer and half-space are considered to be homogeneous elastic media. Theoretical background for the physics of the problem is provided by presenting the fundamentals of elastic wave propagation with specialization to the Love wave case and by a statement of the physical nature and mathematical form of applicable boundary conditions. Interest is focused on the amplitudes of the transmitted and reflected Love waves relative to the magnitude of the excitation, i.e., the transmission and reflection coefficients, for a range of both the "strength" of the discontinuity (magnitude of change in thickness relative to layer thickness) and the layer thickness. The analysis employs scattered fields in the form of integrals in the complex plane; boundary conditions are applied to the total fields. To satisfy the resulting equations for the boundary conditions, the nature of some of the unknown coefficients in the scattered field integrals is postulated and a function-theoretic argument is employed to determine these coefficients. The transmission and reflection coefficients are then extracted by a standard appeal to the calculus of residues and the energy contained in the diffracted fields is evaluated. Both displacement amplitude and energy coefficients are displayed graphically as a function of the parameters h and H. The results presented show that the reflected energy constitutes less than one percent of the incident energy for all crust thicknesses considered

here. The amplitude transmission coefficient relating the relative magnitude of the displacements of the transmitted and incident waves is shown to take on values greater than unity for low frequency and an energy analysis shows that this behavior does not violate the principle of energy conservation. A comparison reveals that the results shown here are in close agreement with those given by Knopoff and Hudson (reference 8). However, a discrepancy does exist for intermediate values of crust thickness and is discussed in some detail.

LIST OF FIGURES

TABLE OF CONTENTS

I

INTRODUCTION

Recently, considerable progress has been made in the theoretical analysis of wave characteristics of various complicated structures that approximate seismic discontinuities. Beyond the results that they can supply, these analyses are important both as an indication of their usefulness in examining other problems, and as groundwork for an insight into more physically realistic situations. The problem considered here is that of Love wave propagation in a surface layer over a half-plane substratum. The object of the analysis is the determination of the amplitude coefficients and energy associated with the transmitted and reflected Love waves which occur when a Love wave is incident upon a discontinuity in the layer. The topic is of considerable geophysical interest because it is an approximate model of seismic wave interaction with the continental margin and other discontinuities in the earth's crust. Although the problem has been considered by other authors, e.g., references 8 and 13, in most cases these analyses lack graphical results or include approximations which limit the range of accuracy.

A geometrical model for the problem is shown in Figure 1; a fundamental mode Love wave, propagating toward the right in the surface layer, or crust, of thickness h, encounters a discontinuity where the surface layer thickness becomes h + H. Rigidities, densities, and velocities of shear waves are taken as μ_1, ρ_1, β_1 in the surface layer and μ_2, ρ_2, β_2 in the semi-infinite substratum or mantle. The region above

the crust is taken to be free space. It will be shown later that, in order for a Love wave to exist in this crust-mantle structure, β_2 and μ_2 must be greater than β_1 and μ_1, respectively. The origin of coordinates is taken at the lower edge of the step change in crust thickness, the positive x direction being the direction of propagation and the z-axis pointing into the mantle.

Unfortunately, the geometry of Figure 1 leads to a difficult boundary value problem. In order to facilitate a solution, a modification of the geometry identical to that used by Kane (reference 7) is applied to the structure. It is felt that this modification alters the problem only slightly for small changes in layer thickness. The free surface boundary $x = o, -H \leq z \leq 0$ is extended back to $x = -\infty$ as shown in Figure 2. In order to preserve the free surface of the layer for $x < 0$, this extension is performed in such a fashion that there is infinitesimal separation between the newly introduced waveguide and the surface layer of thickness h, i.e., a thin fissure along the negative x-axis that prevents transfer of radiation across that boundary.

Since the wavelengths of seismic vibrations associated with the problem are very long, it is felt that the addition of the new acoustic duct introduces at most only minor perturbations into the problem. Indeed it is to be expected that very little energy would propagate into this duct because the frequencies are in many cases below the cut-off, and because the duct is in the backscattered direction of the assumed excitation.

Finally, the media of both crust and mantle are taken to be isotropic elastic solids. In this case the number of elastic constants

(which in the generalized form of Hooke's law is 36) degenerates to two (page 5 of reference 5), greatly simplifying the stress-strain relations. In Chapter III, the case of slight damping is assumed, but this is solely for temporary mathematical convenience and should not be considered an indication of imperfec_ elasticity.

II

FUNDAMENTALS OF ELASTIC WAVE PROPAGATION

The problem being considered concerns the propagation of elastic waves in isotropic media. Therefore, an outline of the theory of motion in elastic solids and the concomitant equations of motion is pertinent. A classic treatment of the material that follows is found in reference 14.

Consider a point P in a deformable body with retangular coordinates x, y, z being displaced to a new position x + u, y + v, z + w. It is assumed that the displacements are small enough so that second and higher order terms occurring in the stress and strain components may be neglected. Then the general form of the stress-strain component relations becomes linear (reference 14).

From the theory of elasticity, the arrays

$$(1) \qquad \begin{matrix} e_{xx} & e_{xy} & e_{xz} \\ e_{yx} & e_{yy} & e_{yz} \\ e_{zx} & e_{zy} & e_{zz} \end{matrix}$$

and

$$(2) \qquad \begin{matrix} p_{xx} & p_{xy} & p_{xz} \\ p_{yx} & p_{yy} & p_{yz} \\ p_{zx} & p_{zy} & p_{zz} \end{matrix}$$

represent the strain and stress tensors at P, respectively. Since $e_{xy} = e_{yx}$, ... and $p_{xy} = p_{yx}$, ..., these arrays are symmetrical.

If the coordinate system coincides with the principal axes, the shear components of stress and strain vanish. Then the deformation at P is completely specified by the corresponding extensions (neglecting higher order terms)

$$(3) \qquad e_{xx} = \frac{\partial u}{\partial x}, \quad e_{yy} = \frac{\partial v}{\partial y}, \quad e_{zz} = \frac{\partial w}{\partial z}$$

and the stress at P is specified completely by the principal stresses P_{xx}, P_{yy}, P_{zz} corresponding to these axes.

Consider a minute portion of the matter enclosing P which undergoes deformation. The cubical dialation θ is defined (reference 3) as the limit, as the surface area approaches zero, of the proportionate increase in the volume of this matter and is equal to the sum of the principal extensions associated with this deformation:

$$(4) \qquad \theta = e_{xx} + e_{yy} + e_{zz} = \frac{\partial u}{\partial x} + \frac{\partial v}{\partial y} + \frac{\partial w}{\partial z}$$

For a derivation of the equations of motion, consideration is given to the stress components (2) across the surfaces of a volume element with dimensions Δx, Δy, and Δz. The equations are obtained by adding the forces acting on the element and the inertia terms $-\rho \frac{d^2u}{dt^2} \Delta x \Delta y \Delta z, \ldots$, for each component. This summation yields:

$$(5) \qquad \rho \frac{d^2u}{dt^2} = \frac{\partial p_{xx}}{\partial x} + \frac{\partial p_{yx}}{\partial y} + \frac{\partial p_{zx}}{\partial z}$$

$$(6) \qquad \rho \frac{d^2 v}{dt^2} = \frac{\partial p_{xy}}{\partial x} + \frac{\partial p_{yy}}{\partial y} + \frac{\partial p_{zy}}{\partial z}$$

$$(7) \qquad \rho \frac{d^2 w}{dt^2} = \frac{\partial p_{xz}}{\partial x} + \frac{\partial p_{yz}}{\partial y} + \frac{\partial p_{zz}}{\partial z}$$

In these expressions, body forces are assumed to be absent and ρ is the density of the medium.

Assuming that the media involved can be represented by isotropic elastic solids, the stress-strain relations may be written in terms of two elastic constants (in this case the Lamé constants λ and μ are arbitrarily chosen) in the following manner (reference 5):

$$(8) \qquad \begin{aligned} p_{xx} &= \lambda\theta + 2\mu \frac{\partial u}{\partial x} & p_{xy} &= \mu\left(\frac{\partial u}{\partial y} + \frac{\partial v}{\partial x} \right) \\ p_{yy} &= \lambda\theta + 2\mu \frac{\partial v}{\partial y} & p_{yz} &= \mu\left(\frac{\partial v}{\partial z} + \frac{\partial w}{\partial y} \right) \\ p_{zz} &= \lambda\theta + 2\mu \frac{\partial w}{\partial z} & p_{zx} &= \mu\left(\frac{\partial w}{\partial x} + \frac{\partial u}{\partial z} \right) \end{aligned}$$

Using (8) in (5)-(7) results in the equations of motion in terms of the deplacements u, v, and w of a point in an elastic solid:

$$(9) \qquad \rho \frac{\partial^2 u}{\partial t^2} = (\lambda + \mu)\frac{\partial \theta}{\partial x} + \mu \nabla^2 u$$

$$(10) \qquad \rho \frac{\partial^2 v}{\partial t^2} = (\lambda + \mu)\frac{\partial \theta}{\partial y} + \mu \nabla^2 v$$

$$(11) \qquad \rho \frac{\partial^2 w}{\partial t^2} = (\lambda + \mu)\frac{\partial \theta}{\partial z} + \mu \nabla^2 w$$

Note that $\frac{d^2}{dt^2}$ has been replaced by $\frac{\partial^2}{\partial t^2}$ in the left-hand side of (9)-(11).

The justification for this has already been mentioned, i.e., that the second powers and products which constitute the difference between the expressions are assumed to be small - ignoring these products linearizes the differential equations. The theory developed on this basis has been called "infinitesimal strain theory" (reference 3).

It is convenient to express the displacements in terms of a scalar potential ϕ and a vector potential $\bar{\psi}(\psi_1,\psi_2,\psi_3)$ as follows:

$$\bar{s}(u,v,w) = \text{grad } \phi + \text{curl } \bar{\psi}(\psi_1,\psi_2,\psi_3) \tag{12}$$

Substitution of (12) into (4) yields:

$$\theta = \nabla^2\phi \tag{13}$$

An expansion of (12) gives displacement components in terms of ϕ and ψ_i. Substitution of the expression for u from (12) and θ from (13) into (9) gives:

$$\frac{\partial}{\partial x}\left(\rho\frac{\partial^2\phi}{\partial t^2}\right) + \frac{\partial}{\partial y}\left(\rho\frac{\partial^2\psi_3}{\partial t^2}\right) - \frac{\partial}{\partial z}\left(\rho\frac{\partial^2\psi_2}{\partial t^2}\right)$$

$$= (\lambda+\mu)\frac{\partial}{\partial x}\nabla^2\phi + \mu\frac{\partial}{\partial x}\nabla^2\phi + \mu\frac{\partial}{\partial y}\nabla^2\psi_3 - \mu\frac{\partial}{\partial z}\nabla^2\psi_2 \tag{14}$$

This equation and the two others that result from the substitution of (13) and the appropriate component from (12) into (10) and (11) are

satisfied if the functions ϕ and ψ_i are solutions of

$$(15) \qquad \nabla^2\phi = \frac{1}{\alpha^2}\frac{\partial^2\phi}{\partial t^2}, \qquad \nabla^2\psi_i = \frac{1}{\beta^2}\frac{\partial^2\psi_i}{\partial t^2}, \qquad i = 1,2,3$$

where

$$(16) \qquad \alpha = \sqrt{\frac{\lambda+2\mu}{\rho}}, \qquad \beta = \sqrt{\frac{\mu}{\rho}}$$

provided that ρ is independent of the coordinates x, y, and z. Equations (15) are the reduced wave equations, and they indicate that the existence of two types of waves with velocities α and β is possible in an isotropic elastic solid.

BOUNDARY CONDITIONS

Since the problem deals with bounded media, some special conditions expressing the behavior of stresses and displacements at boundaries must be included. In particular, at the free surface of a solid, all stress components must vanish and, assuming that solid media are joined perfectly at the surface of contact, all stress and displacement components are continuous across the interface between two media.

LOVE WAVES

Under the assumptions of small displacements and the absence of body forces the first section of this chapter has shown that two types of disturbances, governed by the wave equations (15) and with velocities given by (16), can travel in a homogeneous isotropic elastic solid.

In addition, the previous section states the conditions that the stress components (8) and/or the displacements are subject to at the boundaries of the media.

The waveform of these disturbances is influenced by the particular geometry of the physical environment. For the stratified structure of this problem, Love (reference 10) has shown that one of the possible disturbances consists of horizontally polarized shear (SH) waves which, in the notation of Figure 1, means that displacements are in the y-direction (v component). Although other types of disturbances are possible in this structure, the concern here is with these SH waves which are called Love waves after the person who provided their explanation.

For monochromatic vibrations, a time factor of $e^{-i\omega t}$ can be suppressed. With u = w = o and the displacements independent of the coordinate y, the equations of motion (5)-(7) reduce to

$$(\nabla^2 + k_{\beta_1}^2)v_1 = 0 \tag{17}$$

for the layer and to

$$(\nabla^2 + k_{\beta_2}^2)v_2 = 0 \tag{18}$$

for the substratum, where

$$k_{\beta_1} = \frac{\omega}{\beta_1}, \qquad k_{\beta_2} = \frac{\omega}{\beta_2} \tag{19}$$

the shear wave velocities β_1 and β_2 being given by the second expression in (16) with μ and ρ subscripted appropriately. For a crust thickness t overlying a halfspace and the coordinate system oriented as in Figure 1, with origin at the free surface, assume displacements of the form

$$v_1 = V_o A(\nu) \cos(s_1 z)\, e^{i\nu x}, \qquad 0 \le z \le t \tag{20}$$

$$v_2 = V_o e^{-s_2(z-t)+i\nu x}, \qquad z > t \tag{21}$$

where

$$s_1 = \nu\gamma_1 = \nu\sqrt{\left(\frac{c}{\beta_1}\right)^2 - 1} = \sqrt{k_{\beta_1}^2 - \nu^2} \tag{22}$$

$$s_2 = \nu\gamma_2 = \nu\sqrt{1 - \left(\frac{c}{\beta_2}\right)^2} = \sqrt{\nu^2 - k_{\beta_2}^2} \tag{23}$$

c = phase velocity of the Love wave

and V_o is an arbitrary amplitude constant. The boundary conditions require that the stress p_{zy} vanish at the free surface z = o and that $(p_{zy})_1 = (p_{zy})_2$, $v_1 = v_2$ at the interface z = t. By (8), with w = o, (20), and (21), application of these conditions results in $A(\nu)=\sec(s_1 t)$ and, for a non-trivial solution, the period equation

$$\tan(s_1 t) = \frac{\mu_2\gamma_2}{\mu_1\gamma_1} = \frac{\mu_2 s_2}{\mu_1 s_1} \tag{24}$$

The real values of ν that satisfy this period equation are the

propagation constants $\nu_n = \frac{\omega}{c_n}$ of the Love wave (Note that $-\nu_n$ are also roots of (24) by virtue of its evenness in ν). Figure 3 shows a plot of the curves representing the right and left hand sides of (24) as a function of the parameter $s_1 t$. The intersections shown by the circles define the values of ν_n which are real roots of the period equation and correspond to the various possible modes in the crust, where c_n is the phase velocity of the $n^{\underline{th}}$ mode. In practical seismology, where much of the total energy is associated with the smaller values of ν_n (longer wavelengths), the fundamental mode ($s_1 t < \pi/2$) is of prime importance. For this problem, the excitation will consist of only this mode. Although the constructed solution will be in general a superposition of all possible diffracted modes, transmission and reflection coefficients for the higher order modes will not be calculated.

The appearance of the radicals s_1 and s_2 in the displacements (20), (21), in the light of (22), (23), and (24) requires that $k_{\beta_2} < \nu_n < k_{\beta_1}$ or $\beta_1 < c < \beta_2$. Also, it can be shown that $\beta_2 < \beta_1$ produces no relevant solutions. From this fact and the expression for β in (16) it is established that the existance of a Love wave is contingent upon $\beta_2, \mu_2 > \beta_1, \mu_1$ respectively.

The phase velocity c is a function of the layer thickness t. Figure 4 shows this functional dependence by a semi-log plot of c/β_1 vs. the parameter νt for the case $\mu_2/\mu_1 = 1.8$, $\beta_2/\beta_1 = 1.29$, where c is the first mode phase velocity. The parameter νt is a measure of crust thickness. As $t \to \infty$, $c/\beta_1 \to 1$, i.e., as the crust becomes a half plane the v_1 portion of the Love wave approaches a plane wave traveling with velocity β_1. On the other hand, as $\nu t \to o$, $c/\beta_1 \to \beta_2/\beta_1$ and the v_2 portion of the wave approaches a plane wave with velocity β_2.

III

CONSTRUCTION OF THE SOLUTION

Now that the form of the elastic disturbance, the stress relations, and the boundary conditions for the problem at hand have been established it is possible to assume a fundamental Love wave excitation and proceed with the solution.

For the structure of Figure 2, this excitation takes the form (omitting $e^{-i\omega t}$)

$$
\begin{aligned}
v_{i1} &= A_i(\alpha) \cos [s_1(\alpha) z]\, e^{i\alpha x}, \quad 0 \le z \le h \\
&\qquad\qquad\qquad\qquad\qquad\qquad\qquad\qquad - \infty < x < \infty \\
v_{i2} &= e^{-s_2(\alpha)(z-h) + i\alpha x}, \quad z > h
\end{aligned}
\tag{25}
$$

where

$$
s_1(\upsilon) = \sqrt{k_{\beta_1}^2 - \upsilon^2}, \quad s_2(\upsilon) = \sqrt{\upsilon^2 - k_{\beta_2}^2}, \quad A_i(\upsilon) = \sec[s_1(\upsilon) h] \tag{26}
$$

The root $\upsilon = \alpha$ of the period equation

$$
\tan[s_1(\upsilon) h] = \frac{\mu_2\, s_2(\upsilon)}{\mu_1\, s_1(\upsilon)} \tag{27}
$$

for $x < 0$ is the propagation constant for this first mode incident wave. As a matter of reference this incident field is assumed to have unit displacement magnitude at the interface $z = h$. Transmitted and reflected

wave amplitudes will be compared with this unit reference.

It should be noted that the period equation (27) for $x < 0$ arises from the stipulation that solutions of the boundary condition equations are non-trivial and is thus an essential aspect of Love wave formulation. Therefore, the transmitted Love wave has a propagation constant $K = \omega/c'$ which is a root of the period equation for the region $x > 0$ where this equation is identical to (27) with h replaced by $h + H$.

As the initial step of the procedure one seeks to add scattered fields v_{s1}, v_{s3} in the crust and v_{s2} in the mantle such that the total fields

$$v_3 = v_{s3}, \quad -H \le x \le 0, \text{ all } x \tag{28}$$

$$v_1 = v_{i1} + v_{s1}, \quad 0 < z \le h, \text{ all } x \tag{29}$$

$$v_2 = v_{i2} + v_{s2}, \quad z > h, \text{ all } x \tag{30}$$

satisfy the homogeneous wave equations

$$(\nabla^2 + k_{\beta_1}^2)\, v_3 = 0, \quad -H \le z \le 0, \text{ all } x \tag{31}$$

$$(\nabla^2 + k_{\beta_1}^2)\, v_1 = 0, \quad 0 < z \le h, \quad \text{all } x \tag{32}$$

$$(\nabla^2 + k_{\beta_2}^2)\, v_2 = 0, \quad z > h, \quad \text{all } x \tag{33}$$

and comply with the demands of the boundary conditions

$$(p_{zy})_1 = (p_{zy})_2, \quad z = h, \quad \text{all } x \tag{34}$$

$$v_1 = v_2, \quad z = h, \quad \text{all } x \tag{35}$$

(36) $(p_{zy})_3 = 0, \quad z = -H, \quad \text{all } x$

(37) $(p_{zy})_3 = 0, \quad z = 0, \quad x < 0$

(38) $(p_{zy})_1 = 0, \quad z = 0, \quad x < 0$

(39) $(p_{zy})_3 = (p_{zy})_1, \quad z = 0, \quad x > 0$

(40) $v_3 = v_1, \quad z = 0, \quad x > 0$

Also, except for the incident fields, v_1, v_2, and v_3 should represent outgoing waves and be bounded and continuous at the origin or edge of the fissure.

Arbitrary solutions of the reduced wave equations (31)-(33) can be written as follows:

(41) $$v_{s1} = \frac{1}{2\pi i} \int_C \left[\frac{C(\nu) \sin [s_1(z-h)]}{s_1 \cos s_1 h} + \frac{D(\nu) \cos [s_1(z-h)]}{s_1 \sin s_1 h} \right] e^{i\nu x} \, d\nu$$

(42) $$v_{s2} = \frac{1}{2\pi i} \int_C \frac{F(\nu)}{\delta(\nu)} e^{-s_2(z-h) + i\nu x} d\nu$$

(43) $$v_{s3} = -\frac{1}{2\pi i} \int_C \frac{B(\nu) \cos [s_1(z+H)]}{s_1 \sin s_1 H} e^{i\nu x} \, d\nu$$

where

(44) $$\delta(\nu) = s_1 \sin s_1 h - \frac{\mu_2}{\mu_1} s_2 \cos s_1 h$$

and s_1, s_2 are given by (26). The coefficients $B(\nu)$, $C(\nu)$, $D(\nu)$, and $F(\nu)$ are unknown functions of ν and C is some contour in the complex ν-plane.

At first it seems that the form of (41)-(43) introduces undue complexity into the mathematics but it will be seen that these expressions lead to simple boundary condition equations, thus facilitating solutions for the unknown coefficients.

It is mathematically convenient to assume a small imaginary part, proportional to $e^{i\epsilon}$, in the propagation constants k_{β_1}, k_{β_2} and in the roots α, K associated with the regions $x < 0$ and $x > 0$ respectively; that is,

$$k_{\beta_1} = |k_{\beta_1}|e^{i\epsilon} , \qquad k_{\beta_2} = |k_{\beta_2}|e^{i\epsilon}$$

(45)

$$\alpha = |\alpha|e^{i\epsilon} , \qquad K = |K|e^{i\epsilon}$$

This assumption causes the fields to possess a slight attenuation in the direction of propagation; in the final analysis ϵ will be set equal to zero. Vertical branch cuts from the branch points $\pm k_{\beta_2}$ are so chosen that the cut ν-plane shown in Figure 5 represents that sheet of the Riemann surface for which $\mathrm{Re}\sqrt{\nu^2 - k_{\beta_2}^2} \geq 0$.

By (8) with $p_{zy} = p_{yz}$, application of the boundary conditions (34)-(40) to the total fields (28)-(30) yields, from (34):

$$(46) \qquad \frac{1}{2\pi i}\int_c \left[\frac{\mu_1 C(\nu)}{\cos s_1 h} + \frac{\mu_2 s_2 F(\nu)}{\delta(\nu)} \right] e^{i\nu x}\, d\nu = 0, \quad -\infty < x < \infty$$

from (35):

$$(47) \qquad \frac{1}{2\pi i}\int_c \left[\frac{D(\nu)}{s_1 \sin s_1 h} - \frac{F(\nu)}{\delta(\nu)} \right] e^{i\nu x}\, d\nu = 0, \quad -\infty < \infty < \infty$$

The form of v_{s3} is such that (36) is identically satisfied.

From (37):

$$(48) \qquad \frac{1}{2\pi i}\int_c \mu_1 B(\nu)\, e^{i\nu x}\, d\nu = 0, \quad x < 0$$

from (38):

$$(49) \qquad \frac{1}{2\pi i}\int_c \mu_1 \left[C(\nu) + D(\nu)\right] e^{i\nu x}\, d\nu = 0, \quad x < 0$$

from (39):

$$(50) \qquad \frac{1}{2\pi i}\int_c \left[B(\nu) - C(\nu) - D(\nu)\right] e^{i\nu x}\, d\nu = 0, \quad x > 0$$

Finally, the condition that expresses continuity of displacement at $z = 0$, $x > 0$ includes a non-zero contribution from the incident Love wave. For x positive, this excitation can be written

$$(51) \qquad v_{i1} = \frac{1}{2\pi i}\int_c \frac{A_i(\alpha)\cos[s_1(\alpha)z]}{\nu-\alpha}\, e^{i\nu x}\, d\nu$$

$$(52) \qquad v_{i2} = \frac{1}{2\pi i}\int_c \frac{e^{-s_2(\alpha)(z-h)}}{\nu-\alpha}\, e^{i\nu x}\, d\nu$$

by the Cauchy Integral Theorem. The boundary condition (40) yields:

$$(53)\ \frac{1}{2\pi i}\int_{C^-}\left[-\frac{B(\nu)\cot s_1 H}{s_1} - \frac{A_i(\alpha)}{\nu-\alpha} + \frac{C(\nu)\tan s_1 h - D(\nu)\cot s_1 h}{s_1}\right] e^{i\nu x}d\nu = 0,$$

for $x > 0$.

A beginning toward satisfying the above integral equations (46)-(50) and (53), is found by postulating the nature and behavior of some of the coefficients in certain regions of the ν-plane. Equation (48) is satisfied if $B(\nu)$ is analytic for $\mathrm{Im}\nu < |k_{\beta_2}| \sin\epsilon$ and is of the order $\nu^{-\epsilon_1}$ ($\epsilon_1 > 0$) as $|\nu| \to \infty$ in the specified half-plane of analyticity. Then the integral will vanish by Jordan's Lemma (reference 9). This postulated behavior is denoted by writing $B(\nu)$ as $B^-(\nu)$. Equations (49) and (50) are satisfied if

$$(54)\qquad C(\nu) + D(\nu) = B^-(\nu)$$

Consider next (46) and (47) which hold for all x. Equating the integrands to zero and solving for $C(\nu)$ and $D(\nu)$ yields:

$$(55)\qquad C(\nu) = -\frac{\mu_2}{\mu_1}\frac{s_2\cos s_1 h}{\delta(\nu)}F(\nu)$$

$$(56)\qquad D(\nu) = \frac{s_1\sin s_1 h}{\delta(\nu)}F(\nu)$$

Inserting the expressions into (54) with $\delta(\nu)$ given by (44) results in:

$$(57)\qquad F(\nu) = \Sigma^-(\nu)$$

Thus, $F(\nu)$ has the same behavior as $B^-(\nu)$ for $\mathrm{Im}\nu < |k_{\beta_2}| \sin\epsilon$, i.e., $F(\nu) \triangleq F^-(\nu)$. The last equation to be satisfied is (53). With $F(\nu) = B^-(\nu)$ and $C(\nu)$ and $D(\nu)$ given by (55) and (56), (53) then becomes

$$(58) \qquad \frac{1}{2\pi i}\int_c G(\nu)e^{i\nu x}d\nu = 0, \quad x > 0$$

where

$$(59) \qquad G(\nu) = -\frac{A_i(\alpha)}{\nu-\alpha} + \left[-\frac{\cot s_1 H}{s_1} - \frac{\mu_2 s_2 \sin s_1 h}{\mu_1 s_1 \delta(\nu)} - \frac{\cos s_1 h}{\delta(\nu)}\right]B^-(\nu)$$

This last boundary condition equation is satisfied if $G(\nu)$ is analytic for $\mathrm{Im}\nu > -|k_{\beta_2}| \sin\epsilon$ and is of the order $\nu^{-\epsilon_2}(\epsilon_2 > 0)$ as $|\nu| \to \infty$ in this half plane. This behavior is denoted by writing $G(\nu)$ as $G^+(\nu)$.

Now the problem becomes that of solving for the unknown coefficients of the scattered fields, particularly $B^-(\nu)$ which has the postulated behavior.

Since (59) is the only expression available for the extraction of the unknowns it becomes necessary to introduce a function-theoretic argument based on the Wiener-Hopf technique (reference 12). For convenience let

$$(60) \qquad \Sigma(\nu) = -\frac{\cot s_1 H}{s_1} - \frac{\mu_2 s_2 \sin s_1 h}{\mu_1 s_1 \delta(\nu)} - \frac{\cos s_1 h}{\delta(\nu)}$$

Provided that it has certain properties, $\Sigma(\nu)$ may be expressed as (references 2, 11, 12, and 16,)

$$\Sigma(\nu) = \frac{\sigma^{+}(\nu)}{\sigma^{-}(\nu)} \tag{61}$$

where

1. $\sigma^{+}(\nu)$ is regular and zeroless for $\mathrm{Im}\nu > -|k_{\beta_2}| \sin\epsilon$.

2. $\sigma^{-}(\nu)$ is regular and zeroless for $\mathrm{Im}\nu < |k_{\beta_2}| \sin\epsilon$.

3. $|\sigma^{+}(\nu)|, |\sigma^{-}(\nu)|$ lie between positive bounds in their respective domains of regularity as $|\nu|$ becomes large.

Consequently, (59) can be rewritten, on dividing through by $\sigma^{+}(\nu)$, as

$$\frac{G^{+}(\nu)}{\sigma^{+}(\nu)} + \frac{A_i(\alpha)}{(\nu-\alpha)\,\sigma^{+}(\nu)} = \frac{B^{-}(\nu)}{\sigma^{-}(\nu)} \tag{62}$$

Subtracting $\dfrac{A_i(\alpha)}{(\nu-\alpha)\,\sigma^{+}(\alpha)}$ from each side gives

$$\frac{G^{+}(\nu)}{\sigma^{+}(\nu)} + \frac{A_i(\alpha)}{\nu-\alpha}\left[\frac{1}{\sigma^{+}(\nu)} - \frac{1}{\sigma^{+}(\alpha)}\right] = \frac{B^{-}(\nu)}{\sigma^{-}(\nu)} - \frac{A_i(\alpha)}{(\nu-\alpha)\,\sigma^{+}(\alpha)} \tag{63}$$

An inspection of (63) reveals that the left hand side is regular for $\mathrm{Im}\nu > -|k_{\beta_2}| \sin\epsilon$ and the right hand side is regular for $\mathrm{Im}\nu < |k_{\beta_2}| \sin\epsilon$. In addition, because of the assumed growths of $G^{+}(\nu)$ and $B^{-}(\nu)$ for large $|\nu|$, these functions tend to zero as $|\nu| \to \infty$ in their respective half planes.

By the previous paragraph and the overlapping regions of regularity shown in Figure 5, each side of (63) is the analytic continuation of the other (reference 15) and thus defines an entire function. Invoking the Liouville Theorem (reference 4) in the light of the prescribed

behavior at $|\nu| = \infty$, each side of (63) can be equated to zero, giving

$$(64) \qquad G^+(\nu) = \frac{A_i(\alpha)}{\nu - \alpha}\left[\frac{\sigma^+(\nu)}{\sigma^+(\alpha)} - 1\right]$$

$$(65) \qquad B^-(\nu) = \frac{A_i(\alpha)\,\sigma^-(\nu)}{(\nu-\alpha)\,\sigma^+(\alpha)} = \frac{\sigma^+(\nu)\,A_i(\alpha)}{\sigma^+(\alpha)\,(\nu-\alpha)\,\Sigma(\nu)}$$

The diffracted fields can now be specified completely via substitution of (65) and (55)-(57) into (41)-(43), and the total fields (28)-(30) become

$$(66) \quad v_3 = -\frac{1}{2\pi i}\int_c \frac{\sigma^+(\nu)}{\sigma^+(\alpha)}\,\frac{A_i(\alpha)\,\cos\,[s_1(z+H)]}{(\nu-\alpha)\Sigma(\nu)s_1\,\sin\,s_1H} - e^{i\nu x}\,d\nu, \quad -H \le z \le 0$$

$$(67) \quad v_1 = v_{i1} + \frac{1}{2\pi i}\int_c \frac{\sigma^+(\nu)}{\sigma^+(\alpha)}\,\frac{A_i(\alpha)}{(\nu-\alpha)\Sigma(\nu)\delta(\nu)}\left[\cos[s_i(z-h)] - \frac{\mu_2 s_2}{\mu_1 s_1}\sin[s_1(z-h)]\right]e^{i\nu x}d\nu,$$

$$0 \le z \le h$$

$$(68) \quad v_2 = v_{i2} + \frac{1}{2\pi i}\int_c \frac{\sigma^+(\nu)}{\sigma^+(\alpha)}\,\frac{A_i(\alpha)}{(\nu-\alpha)\Sigma(\nu)\delta(\nu)}\,e^{-s_2(z-h)+i\nu x}\,d\nu.$$

IV

THE TRANSMISSION AND REFLECTION COEFFICIENTS

Evaluation of Total Fields

The integral expressions for the total fields (66)-(68) can, at least in principle, be evaluated by a standard method. For the Love waves, depending on whether the transmitted ($x > 0$) or reflected ($x < 0$) field is being considered, the contour C along the real axis is closed in the appropriate half plane by an infinite arc with due regard being taken not to cross the branch cuts emanating from the branch points $\pm k_{\beta_2}$. By Jordan's Lemma the integral along the infinite arc makes no contribution so that by the Residue Theorem (reference 4) the closed contour integral can be expressed as follows:

$$(69) \qquad \int_{\substack{\text{closed}\\ \text{contour}}} = \int_C + \int \text{branch cut} = \pm 2\pi i \sum \text{residues}.$$

The branch cut integral can be evaluated by the method of saddle points. The resultant field is the SH cylindrical body waves that are scattered into the mantle and will not be discussed. Therefore, by (69) the scattered surface waves of interest are obtained as the residue fields of the closed contour integral.

For the transmitted field, application of Jordan's Lemma requires that the contour be closed in the upper half plane. Letting ϵ shrink to zero, the contour C is deformed below singularities for $\mathrm{Re}\nu > 0$

and above these singularities for Reν < 0 as shown in Figure 5. This contour and the upper half-plane with both Reimann sheets displayed is shown in Figure 6. The period equation for the region x > 0 is included in $\Sigma(\nu)$ (see equation 3, Appendix A) and produces a pole of the integrands of (66)-(68) at $\nu = \pm K$ provided that the radical $s_2 = \sqrt{\nu^2 - k_{\beta_2}^2}$ is positive real. Therefore, the poles $\pm K$ lie on the sheet that extends from the upper left to lower right of Figure 6 where $\mathrm{Re}\sqrt{\nu^2 - k_{\beta_2}^2} > 0$ in general, and where $\sqrt{\nu^2 - k_{\beta_2}^2}$ is for positive real for ν real and greater than k_{β_2}.

The integrand in (66) has no other poles, but those in (67) and (68) have poles at $\nu = \pm \alpha$ provided that s_2 has the same sign as before, as can be seen from the period equation (27) for the thinner layer. That these poles at $\pm \alpha$ exist is shown as follows: Expressing $\delta(\nu)$ as

$$\delta(\nu) = - s_1 \cos s_1 h \left[\frac{\mu_2 s_2}{\mu_1 s_1} - \tan s_1 h\right] \tag{70}$$

from (44) and considering the product $(\nu-\alpha)\Sigma(\nu)\delta(\nu)$, one sees that there is a cancellation of the period equation in h between the denominator of $\Sigma(\nu)$ (see equation 3, Appendix A), and $\delta(\nu)$, leaving the linear factor $(\nu-\alpha)$, thus giving a pole at $\nu = \alpha$. For the pole at $\nu = -\alpha$, consider $\Sigma(\nu)$ as the quotient $\frac{\sigma^+(\nu)}{\sigma^-(\nu)}$. Then,

$$\frac{\sigma^+(\nu)}{\sigma^-(\alpha)} \frac{A_i(\alpha)}{(\nu-\alpha)\Sigma(\nu)\delta(\nu)} = \frac{\sigma^-(\nu)}{\sigma^+(\alpha)} \frac{A_i(\alpha)}{(\nu-\alpha)\delta(\nu)} \tag{71}$$

and $\delta(\nu)$ contains the pole at $\nu = -\alpha$.

The pole at $\nu = -\alpha$ is associated with the reflected wave. In this case, the application of Jordan's Lemma requires that the contour be closed in the lower half ν-plane. This suitably indented contour, both Riemann sheets of the lower half ν-plane, and the pole at $\nu = -\alpha$ are shown in Figure 7. The sheets in this figure are oriented as in Figure 6, i.e., Re $s_2 \geq 0$ on the sheet extending from upper left to lower right. This orientation does not imply that the two sheets have the entire branch cut in common. In fact, only the branch <u>point</u> is common to both sheets.

It must be noted that no mention has been made of the singularities of $\sigma^+(\nu)$ and $\sigma^-(\nu)$. Although both these factors contain singularities, they are used in the integrals so that these singularities are not included within the contours of Figures 6 and 7. The transmitted field integrand contains $\sigma^+(\nu)$ which is regular and zeroless in the upper half ν-plane, which is the region enclosed by the contour of Figure 6. For the reflected field, the integrand may be altered by use of (71) and the term $\sigma^-(\nu)$ presents no singularities within the contour of Figure 7.

The specification of contours and location of poles makes it possible to extract the residue fields. Noting that the residue associated with the pole $\nu = +\alpha$ serves only to cancel the incident Love wave in the region $x > 0$ (which is to be expected since the Love wave cannot propagate undisturbed past the discontinuity), the transmitted fields are

$$(72)\quad v_{t1} = T_1(k_{\beta_1}, k_{\beta_2}, h, H)\left\{\cos[s_1(K)(z-h)] - \frac{\mu_2 s_2(K)}{\mu_1 s_1(K)} \sin[s_1(K)(z-h)]\right\} e^{iKx},$$

$$0 \leq z \leq h$$

(73) $v_{t2} = T_2(k_{\beta_1}, k_{\beta_2}, h, H)\, e^{-s_2(K)(z-h) + iKx}, \quad z > h$

(74) $v_{t3} = T_3(k_{\beta_1}, k_{\beta_2}, h, H) \cos [s_1(K)(z + H)]\, e^{iKx}, \quad -H \le z \le 0$

where the transmission amplitude coefficients T_1, T_2, T_3, can be calculated as

(75) $$T_1 = T_2 = \frac{\sigma^+(K)}{\sigma^+(\alpha)} \frac{A_i(\alpha)}{(K-\alpha) \frac{d}{d\nu} \Sigma(\nu)\Big|_{\nu=K} \delta(K)}$$

(76) $$T_3 = - \frac{\sigma^+(K)}{\sigma^+(\alpha)} \frac{A_i(\alpha)}{(K-\alpha) \frac{d}{d\nu} \Sigma(\nu)\Big|_{\nu=K} s_1(K) \sin [s_1(K)H]}$$

with $s_1(K) = \sqrt{k_{\beta_1}^2 - K^2}$, $s_2(K) = \sqrt{K^2 - k_{\beta_2}^2}$

The reflected fields are

(77) $v_{r1} = R_1(k_{\beta_1}, k_{\beta_2} h, H)\{\cos [s_1(-\alpha)(z-h)] - \frac{\mu_2 s_2(-\omega)}{\mu_1 s_1(-\alpha)} \sin[s_1(-\alpha)(z-h)]\} e^{-i\alpha x}, \quad 0 \le z \le h$

(78) $v_{r2} = R_2(k_{\beta_1}, k_{\beta_2}, h, H)\, e^{-s_2(-\alpha)(z-h) - \alpha x}, \quad z > h$

where, by virtue of equation 15, Appendix A, the reflection amplitude coefficients R_1, R_2 are:

(79) $$R_1 = R_2 = 2 \sqrt{\frac{-\alpha - i|k_{\beta_2}|\sin\epsilon}{\alpha + i|k_{\beta_2}|\sin\epsilon}} \frac{1}{[\sigma^+(\alpha)]^2} \frac{A_i(\alpha)}{2\alpha \frac{d}{d\nu} \delta(\nu)\Big|_{\nu=-\alpha}}$$

with $s_1(-\alpha) = \sqrt{k_{\beta_1}^2 - \alpha^2}$, $s_2(-\alpha) = \sqrt{\alpha^2 - k_{\beta_2}^2}$.

The derivatives in (75), (76), and (79) are as follows:

$$(80)\ \frac{d}{d\nu}\Sigma(\nu) = \frac{1}{\nu^2}\left\{-\left[\frac{\nu H \cos^2 s_1 H}{\gamma_1^2} + \frac{\cot s_1 H}{\gamma_1^3}\right] + \frac{\mu_2}{\mu_1}\left[\frac{\nu h \frac{s_2}{s_1}\cos s_1 h - \sin s_1 \frac{h}{\gamma_2}}{s_1\,\delta(\nu)/\nu^2} + \right.\right.$$

$$+ \frac{s_2}{s_1}\frac{\sin s_1 h\left[\gamma_1 \frac{d}{d\nu}\delta(\nu) - \frac{1}{\gamma_1}\delta(\nu)\right]}{\gamma_1^2[\delta(\nu)]^2/\nu^2}\Big] - \Big[\frac{\nu h \sin s_1 h}{\delta(\nu)/\nu} +$$

$$\left.\left. + \frac{\frac{d}{d\nu}\delta(\nu)\cos s_1 h}{[\delta(\nu)]^2/\nu^2}\right]\right\}$$

$$(81)\ \frac{d}{d\nu}\delta(\nu) = -\left\{\nu h \cos s_1 h + \frac{1}{\gamma_1}\sin s_1 h + \frac{\mu_2 s_2}{\mu_1 s_1}\nu h \sin s_1 h + \right.$$

$$\left. + \frac{\mu_2}{\mu_1}\frac{\cos s_1 h}{\gamma_2}\right\}$$

where γ_1, γ_2 are given in (22) and (23).

Energy Considerations

For a Love wave in the fundamental mode, the rate of energy which passes a plane perpendicular to the x-axis, per unit area, per unit time is (reference 13)

$$(82)\qquad E = \pm\mu \frac{\partial v}{\partial x}\frac{\partial v}{\partial t}$$

where the minus sign is used for propagation in positive x direction and the plus sign for propagation in the opposite direction. For a certain

with $s_1(-\alpha) = \sqrt{k_{\beta_1}^2 - \alpha^2}$, $s_2(-\alpha) = \sqrt{\alpha^2 - k_{\beta_2}^2}$.

The derivatives in (75), (76), and (79) are as follows:

$$(80)\quad \frac{d}{dv}\Sigma(v) = \frac{1}{v^2}\left\{-\left[\frac{vH\cos^2 s_1H}{\gamma_1^2} + \frac{\cot s_1H}{\gamma_1^3}\right] + \frac{\mu_2}{\mu_1}\left[\frac{vh\frac{s_2}{s_1}\cos s_1h - \sin s_1\frac{h}{\gamma_2}}{s_1\,\delta(v)/v^2} + \right.\right.$$

$$+ \frac{s_2}{s_1}\frac{\sin s_1h\left[\gamma_1\frac{d}{dv}\delta(v) - \frac{1}{\gamma_1}\delta(v)\right]}{\gamma_1^2[\delta(v)]^2/v^2}\left.\right] - \left[\frac{vh\sin s_1h}{\delta(v)/v}\frac{1}{\gamma_1} + \right.$$

$$\left.\left. + \frac{\frac{d}{dv}\delta(v)\cos s_1h}{[\delta(v)]^2/v^2}\right]\right\}$$

$$(81)\quad \frac{d}{dv}\delta(v) = -\left\{vh\cos s_1h + \frac{1}{\gamma_1}\sin s_1h + \frac{\mu_2 s_2}{\mu_1 s_1}vh\sin s_1h + \right.$$

$$\left. + \frac{\mu_2}{\mu_1}\frac{\cos s_1h}{\gamma_2}\right\}$$

where γ_1, γ_2 are given in (22) and (23).

Energy Considerations

For a Love wave in the fundamental mode, the rate of energy which passes a plane perpendicular to the x-axis, per unit area, per unit time is (reference 13)

$$(82)\qquad E = \pm\mu\frac{\partial v}{\partial x}\frac{\partial v}{\partial t}$$

where the minus sign is used for propagation in positive x direction and the plus sign for propagation in the opposite direction. For a certain

period $T=2\pi/\omega$ the energy flow is

$$\bar{E} = \int_0^T E\,dt \tag{83}$$

and the total flux across a vertical plane of unit breadth in a period T is

$$[T.F.] = \int_0^\infty \bar{E}\,dz \tag{84}$$

Expressing the incident field as the real part of (25) with the time factor $e^{-i\omega t}$ included yields:

$$v_{i1} = A_i \cos s_1 z \cos(-\omega t + \alpha x), \quad 0 \le z \le h \tag{85}$$

$$v_{i2} = e^{-s_2(z-h)} \cos(-\omega t + \alpha x), \quad z > h \tag{86}$$

where s_1 and s_2 are understood to be $s_1(\alpha)$ and $s_2(\alpha)$, respectively, and $A_i = A_i(\alpha)$ (see (26)). The energy rate per unit time and area of the incident wave is then

$$E_{i1} = A_i^2 \alpha\omega\mu_1 \cos^2 s_1 z \sin^2(-\omega t + \alpha x) \tag{87}$$

for the crust, and

$$E_{i2} = \alpha\omega\mu_2 e^{-2s_2(z-h)} \sin^2(-\omega t + \alpha x) \tag{88}$$

for the mantle. Integrating over a period T gives

(89) $$\bar{E}_{i1} = \pi \alpha \mu_1 A_i^2 \cos^2 s_1 z$$

and

(90) $$\bar{E}_{i2} = \pi \alpha \mu_2 e^{-2s_2(z-h)}$$

Finally, integration over the vertical coordinate z results in an expression for the total incident flux crossing a vertical plane of unit breadth in time T:

(91) $$[T.F.]_{i1} = \mu_1 \pi A_i^2 \alpha \left[\frac{h}{2} + \frac{\sin 2s_1 h}{4s_1} \right]$$

(92) $$[T.F.]_{i2} = \frac{1}{2} \mu_2 \pi \frac{\alpha}{s_2}$$

(93) $$[T.F.]_{inc.} = [T.F.]_{i1} + [T.F.]_{i2}$$

The expression (77) for the reflected field in the crust can be simplified by substituting the right hand side of (27) with $\nu = -\alpha$ for the quantity $\frac{\mu_2 s_2(-\alpha)}{\mu_1 s_1(-\alpha)}$. This substitution simplifies (77) to

(94) $$v_{r1} = R_1 A_i \cos s_1 z \, e^{-i\alpha x}$$

A comparison of (94) and (78) with (85), respectively, with real parts considered, $R_1 = R_2$, $s_1 = s_1(-\alpha) = s_1(\alpha)$, and $s_2(-\alpha) = s_2(\alpha)$, shows that the reflected fields differ from the incident fields by the coefficient $R_{1,2}$ and the sign of α. The sign is accounted for by the sign selection

in (82). Therefore, it is seen that the reflected energy is equal to the incident energy times, say, R_2^2 , or

$$(95) \qquad \frac{[\text{T. F.}]_{\text{refl.}}}{[\text{T. F.}]_{\text{inc.}}} = R_2^2$$

This concise expression (95) is true only for the case where the incident and reflected fields in question are the same mode.

The analysis (82)-(84) as applied to the transmitted fields is facilitated by again employing the period equation for the region $x > 0$ to simplify (72) to

$$(96) \qquad v_{t1} = T_1 A_i \cos [s_1(z + H)] \, e^{iKx}$$

where

$$(97) \qquad A_t = A_t(K) \cdot \sec [s_1(K)(h + H)]$$

The end result of this energy analysis on (96), (73), and (74) is as follows:

$$(98) \quad [\text{T. F.}]_{t1} = \mu_1 \pi T_1^2 A_t^2 K\{ \frac{h}{2} + \frac{1}{4} \frac{\sin[2 s_1(h + H)] - \sin 2 s_1 H]}{s_1} \}$$

$$(99) \quad [\text{T. F.}]_{t2} = \frac{1}{2} \mu_2 \pi T_2^2 \frac{K}{s_2}$$

$$(100) \quad [\text{T. F.}]_{t3} = \mu_1 \pi T_3^2 K\{ \frac{H}{2} + \frac{1}{4} \frac{\sin 2 s_1 H}{s_1} \cdots \}$$

and the total flux transmitted is equal to the sum of (98),(99), and (100). In these transmitted flux expressions, s_1, s_2 are understood to be $s_1(K)$, $s_2(K)$, respectively.

Of interest here are the energies contained in the reflected and transmitted Love waves as a fraction of the energy in the incident Love wave. This ratio for the reflected wave is given by (95). The ratio for the transmitted wave is readily obtainable from the above expressions and is not written here due to the space involved.

Graphical Results

Up to this point, the theory, its application, and the resulting expressions for amplitude coefficients of and flux contained in the various fields can have at most a pseudo-importance and conjectured validity. It may be impressive to display the analysis, concluding with a peremptory statement such as "these expressions are the ---", but the work is neither practical nor believable until the magnitudes of the coefficients and energy ratios are known as a function of the physical parameters h and H.

The proceeding graphs display the quantities that are felt to be of prime importance. All major calculations were performed on the IBM digital computer at the University of Rhode Island. Numerical computation requires that the values of $\frac{\mu_2}{\mu_1}$ and $\frac{\beta_2}{\beta_1}$ be specified. For the purpose of future comparisons with other authors, the values stated in Figure 4 are used.

The calculations of T_i, i = 1,2,3, and R_i, i = 1,2 requires that consideration be given to magnitude only, phase being ommitted, for the expressions representing these coefficients contain terms which are

is in the shadow zone of the incident wave. Also, for the transmitted wave in the fundamental mode, $s_1(K)(h+H) < \pi/2$, so that one is inclined to believe that $s_1(\nu)H$ will remain less than $\pi/2$ at least for fairly small H. This would restrict the value of n in (102) to zero, i.e., the propagation would be analogous to the TEM electromagnetic wave in a parallel plate waveguide. Therefore, it is felt that any propagation along the duct for small H will constitute only a very small percentage of the energy associated with the original problem of Figure 1. Indeed, no unusual behavior is observed in T_2 for $k_{\beta_1} H > 3$, although there is no criterion to determine either the accuracy of the results for large discontinuities or the dividing line between valid and invalid ranges $k_{\beta_1} H$.

Note that $|T_2|$ takes on values greater than unity when the crust thickness for $x < 0$ is small ($k_{\beta_1} h = .05$). However, this unusual behavior is justified by a plot of the ratio of transmitted to incident flux TFT/TFI shown in Figure 10 for the smaller layer thicknesses of Figure 8. This figure verifies the fact that coefficients larger than unity are not necessarily in violation of conservation of energy. In fact, Knopoff and Hudson (reference 8) have shown that the rate of energy transmission in a Love wave is inversely proportional to layer thickness for small frequencies ($k_{\beta_1} h = \frac{\omega h}{\beta_1} \to 0$). It follows that a coefficient associated with transmission from a thin layer to a slightly thicker one which is greater than unity is consistent with energy conservation principles for this range of small frequencies.

Figure 10 indicates that for $k_{\beta_1} h > 2.040$, the rate of change

of the transmitted to incident energy ratio is at first rapid and then diminishes to an almost constant value.

Since $|R_2|$ is small, the normalized reflected energy is negligible (< 1 percent) and will not be displayed.

Knopoff and Hudson have presented an approximate solution to the problem dealt with here (reference 8). Their results are plotted as a function of the crust thicknes $k_{\beta_1}(h+H)$ for $x > 0$ with the ratio of crust thickness for $x < 0$ to crust thickness for $x > 0$ $(\frac{h}{h+H})$ held constant. The incident Love wave in their paper has unit amplitude at the free surface of the crust and the coefficient calculated is the free surface amplitude of the transmitted Love wave. In this thesis the equivalent quantity is readily obtained as $|T_3|$ divided by $A_i(\alpha)$, and will be denoted by $|TT|$. The method of plotting is as follows: The growth of the crust is such that the ratio of thin to thick layers remains constant, and the curves are shown as a function of the crust thickness $k_{\beta_1}(h+H)$ for $x > 0$. Figure 11 is a comparison of the results of Knopoff and Hudson and this author for ratios of incident to transmitted layer thickness $\frac{h}{h+H}$ of 0.9, 0.8, and 0.7. Note that the results agree with 10 percent for $k_{\beta_1}(h+H) > 5$, and that the limiting values as $k_{\beta_1}(h+H) \to 0$ are coincident. For $k_{\beta_1}(h+H) > 9$, the curves become asymptotic to the dashed lines shown in the figure.

In order to profit from this comparison it is necessary to be aware of any assumptions and the corresponding errors involved in the method of knopoff and Hudson. Only then can the comparison become a gauge to measure the quality of the results of this thesis.

First of all, the displacements along the aperture plane $x = 0$, $0 \leq z \leq \infty$ were assumed, by Knopoff and Hudson, to be those due to the incident wave alone. This assumption is accurate as long as the discontinuity is negligible with respect to the wavelength of incident field. A small or "weak" discontinuity neither converts appreciable energy to SH body waves nor needs to create evanescent modes to effect the transition from incident to transmitted Love waves. Also, from Figure 9, the reflected wave is too small to introduce appreciable error. Therefore, the dashed line curves of Figure 11 can be considered very accurate as $k_{\beta_1}(h+H) \to 0$, for $k_{\beta_1} H \to 0$ simultaneously.

The quantitative effect of the above-mentioned assumption for large crust thickness is not so easily determined. Of all the disturbances associated with the problem, i.e., reflected wave, SH body waves, and evanescent modes, only the first can now be considered negligible. It is suspected that there is some conversion to body waves, but the magnitude and direction of these body wave displacements are unknown. The existance of evanescent modes is also suspected, and again, the magnitudes of these modes are unknown. An indication of a smooth transition from incident to transmitted Love wave is obtained from Figure 4. This figure shows that the Love wave phase velocity is practically invariant with crust thickness for large thicknesses, inferring that the Love wave is relatively unaffected by the discontinuity. Nevertheless, the above statements lead one to be skeptical about the accuracy of Knopoff's and Hudson's results for $k_{\beta_1}(h+H) > 6$. On the other hand, it is felt that the dashed curves of Figure 11 are a fair approximation to the desired coefficient for large crust thickness.

Finally, the assumption under consideration is probably least valid for intermediate crust thickness. In addition to the existance of evanescent and body wave disturbances along the aperture plane, Figure 4 shows that the phase velocity changes considerably for a small change in crust thickness, thus indicating a rough and complex transition from incident to transmitted wave. These conditions imply that the intermediate crust thickness coefficients of Knopoff and Hudson are only rough approximations.

The second assumption of Knopoff and Hudson is that the displacements along the surface $x = 0$, $-H \leq z \leq 0$ are negligible. This heuristic judgement is felt to be valid for at least the small discontinuities associated with Figure 11.

The above discussion and the comparison of Figure 11 establishes the accuracy of the calculated values of this work as $k_{\beta_1}(h+H) \rightarrow 0$ and provides a measure of the accuracy of these calculated values for large $k_{\beta_1}(h+H)$.

Figure 12 shows the coefficient $|T_2|$ in the same manner and for the same values $\frac{h}{h+H}$ as Figure 11. The limiting values as $k_{\beta_1}(h+H) \rightarrow 0$ are the same as those for $|TT|$ curve of Figure 11, finally approaching the dashed lines shown for $k_{\beta_1}(h+H) > 9$.

Again, the validity of the values of $|TT|$ and $|T_2|$ in Figures 11 and 12, at least in terms of energy conservation, can be established by a plot of the fraction of energy contained in the transmitted Love wave vs. $k_{\beta_1}(h+H)$. Figure 13 shows that the coefficients $|TT|$ and $|T_2|$ do satisfy these energy limitations and that the portion of energy transmitted approaches a constant value for large crust thickness.

A final and interesting comparison with the results of Knopoff and Hudson is shown in Figure 14. Calculations were performed on $|TT|$ with the factor $\left|\frac{\sigma+(K)}{\sigma+(\alpha)}\right|$ assumed to have the value unity, and the results were compared with those of the authors mentioned above for the same values of $\frac{h}{h+H}$ as in Figure 11. It is obvious that there is an almost exact correspondence between the results. The above authors have plotted curves for $\frac{h}{h+H} = .9, .8, \ldots . .1$, and although it is not shown here, the equivalence displayed in Figure 14 remains undiminished for each and every value of the ratio of crust thicknesses.

V.

CONCLUSIONS

The conclusions drawn here will be presented in the order of decreasing generality.

Although the first of these conclusions cannot be drawn from the material in this thesis alone, it is included as an indication of the efficacy of the Wiener-Hopf technique.

In the preliminary research connected with this work, exposure to literature including references 1, 4, 6, 10 and 11 has shown that the type of problem amenable by the Wiener-Hopf Technique often contains complicated mixed boundary conditions. The range of this complicated problem is a significant extension beyond that of the simpler problem for which solutions can be obtained by the method of separation of variables. Application of the Wiener-Hopf theory is facilated by variations within the technique and modifications such as the one shown in Figure 2. A typical mixed boundary value problem is that of satisfying the steady-state wave equation in free space when semi-infinite boundaries are present.

The geometry of the problem considered in this thesis is such that the Wiener-Hopf technique is most appropriate for obtaining the transmission and reflection coefficients. Aside from the limitation of absolute values imposed on the coefficients and the ostensibly negligible energy lost via propagation down the duct of Figure 2, the analysis produces accurate results for a large range of crust thicknesses and discontinuity

sizes. A solution by Satō (reference 11) and a modified Green's Theorem approach by Knopoff and Hudson (reference 7) both entail assumptions which either limit the range of results or make them approximate.

A key to evaluation of the results of this thesis lies in the comparisons of Figures 11 and 14. Deviations from the dashed curves of Figure 11 are not important in themselves, for as is shown in the discussion immediately following the introduction of this figure, these curves are approximate. Furthermore, it is suspected that the results of Knopoff and Hudson are too large for intermediate crust thicknesses. As a check, a calculation was performed of TFT/TFI using the amplitude coefficients $|T_2|$ and $|T_3|$ corresponding to Knopoff's and Hudson's approximation (with $\frac{\sigma^+(K)}{\sigma^+(\omega)}$ assumed to be unity). Since the form of the transmitted Love wave in the work of Knopoff and Hudson is equivalent to (72)-(74), this calculation is a test of the accuracy of their results. The resulting values of the energy transmission coefficient TFT/TFI were larger than unity for $.05 < k_{\beta_1}(h+H) < .38$, thus labeling Knopoff's and Hudson's amplitude transmission coefficient as too large for at least this small range of crust thickness.

The approximate nature of Knopoff's and Hudson's results creates the possibility that they are too large for $k_{\beta_1}(h+H) > .38$. Strengthening this possibility is the fact that oversize coefficients may not violate energy restrictions for increasing intermediate crust thickness due to the decreasing behavior of TFT/TFI. Therefore, the fact that the coefficients of Knopoff and Hudson are larger than those of this analysis for $k_{\beta_1}(h+H) < 6$ must in the main be attributed to error on their part.

The solution to the problem considered in this thesis is incomplete insofar as the SH body waves associated with the branch cut integral in (69) have not been discussed. A knowledge of the energy contained in this scattered field would provide an absolute check on the graphical results presented. Although the comparison with Knopoff and Hudson reveals the accuracy of these results, knowledge of this radiated energy completes the picture of energy apportionment. This picture would be a criterion for determining to what degree the modified problem of Figure 2 approximates the original problem, and would establish the maximum H that could be considered.

BIBLIOGRAPHY

1. Angulo, C.M., and W.S.C. Chang,"The Launching of Surface Waves by a Parallel Plate Waveguide," Scientific Report AF 1391/5, Division of Engineering, Brown University, Providence, Rhode Island. April,1957.

2. Bayer, J., and S.N. Karp, "Propagation of Plane Electromagnetic Waves Past a Shoreline," Research Report No. EM-46, Mathematics Research Group, Washington Square College of Arts and Sciences, New York University, New York, New York, November, 1957.

3. Bullen, K.E., An Introduction to the Theory of Seismology, Cambridge University Press, London, 1953.

4. Churchill, R.V., Complex Variables and Applications, McGraw-Hill Book Company, Inc., New York, 1960.

5. Ewing, W.M., W.S. Jardetzky, and F. Press, Elastic Waves in Layered Media, McGraw-Hill Book Company, Inc., New York, 1957.

6. Flugge, S. (ed.), Encyclopedia of Physics, Vol. VI, Springer-Verlag Press, Berlin, 1958.

7. Kane, J. "The Propagation of Rayleigh Waves Past a Fluid-Loaded Boundary," Report 7470/1, Division of Engineering Research and Development, Department of Electrical Engineering, University of Rhode Island, Kingston, Rhode Island, November, 1961.

8. Knopoff, L., and Hudson, "Transmission of Love Waves Past a Continental Margin,"Contribution No. 1209, Division of Geological Sciences, California Institute of Technology, Pasadena, California.

9. LePage, W.R., Complex Variables and the Laplace Transform for Engineers, McGraw-Hill Book Company, Inc., New York, 1961.

10. Love, A.E.H., Some Problems in Geodynamics, Cambridge University Press, London, 1911.

11. Morse, P.M., and H. Feshbach, Methods of Theoretical Physics, Part I, McGraw-Hill Book Company, Inc., New York, 1953.

12. Noble, B., Methods based on the Wiener-Hopf Technique, Pergamon Press, New York 1958.

13. Sato, R. "Love Waves in case the Surface Layer is Variable in Thickness," Journal of Physics of the Earth, Vol. 9, No.2, 1961.

14. Sommerfield, A., Mechanics of Deformable Bodies, Academic Press, Inc. New York, 1950.

15. Thron, W.J., The Theory of Functions of a Complex Variable, John Wiley and Sons, Inc., New York, 1953.

16. Titchmarch, E.C., Theory of Fourier Integrals, Oxford Univ.Press, London, 1948.

APPENDIX A.

FACTORIZATION OF $\Sigma(\nu)$

Introductory Remarks

The integral formulas (66)-(68) are as yet unable to produce explicit expressions for the total field for they contain the arbitrary factors of $\Sigma(\nu)$. There is a general method of factorization (reference 11) which allows a determination of $\sigma^{+}(\nu)$ and $\sigma^{-}(\nu)$ at least as a product of exponentials (with arguments in integral form) and algebraic terms. If the absolute value of these factors is all that need to be determined, then the expressions representing them can be reduced to a form suitable for numerical evaluation.

The method is based on the theorem that a function $q(\nu)$ analytic in the strip $|\mathrm{Im}\nu| < b$ is the sum of two functions, one being analytic for $\mathrm{Im}\nu > -b$, the other for $\mathrm{Im}\nu < b$, and the procedure adopted is the application of Cauchy's Integral Theorem to the boundary of the strip. The integral breaks up into two integrals representing the functions mentioned above. In general, the representation is as follows:

$$q(\nu) = q^{-}(\nu) - q^{+}(\nu) \tag{A-1}$$

where

$$q^{+}(\nu) = \frac{1}{2\pi i}\int_{-\infty-ia}^{\infty-ia} \frac{q(\rho)}{\rho - \nu}\, d\rho \tag{A-2}$$

$$q^{-}(\nu) = \frac{1}{2\pi i}\int_{-\infty+ia}^{\infty+ia} \frac{q(\rho)}{\rho - \nu}\, d\rho$$

$q^+(\nu)$ is analytic for $Im\nu > -a$, while $q^-(\nu)$ is analytic for $Im\nu < a$, and thus $q(\nu)$ is analytic in the strip $|Im\nu| < b$ since a can be chosen as near b as desired.

Application to $\Sigma(\nu)$

Equations (A-1) and (A-2) can be employed to represent $\Sigma(\nu)$ as $\frac{\sigma^+(\nu)}{\sigma^-(\nu)}$ as stated in (61). Since the method produces a sum rather than a product, this is equivalent to breaking up $\ln \Sigma(\nu)$ into $\ln \sigma^+(\nu) - \ln \sigma^-(\nu)$. This may be done as long as $\ln \Sigma(\nu)$ has no singularities in the strip. Since $\Sigma(\nu)$ is analytic in this region by virtue of restriction to the Reimann sheetwhere $Re\sqrt{\nu^2 - k_{\beta_2}^2} > 0$, $\ln \Sigma(\nu)$ possesses the same property there provided that $\Sigma(\nu)$ has no zeros for $|Im\nu| < |k_{\beta_2}| \sin \epsilon$. Manipulation of (60) results in a form which facilitates the location of the roots of $\Sigma(\nu)$. This form is as follows:

$$\text{(A-3)} \qquad \Sigma(\nu) = \frac{1 - \tan s_1 H \tan s_1 h}{s_1 \tan s_1 H \left[\frac{\mu_2 s_2}{\mu_1 s_1} - \tan s_1 h\right]} \left[\tan [s_1(h + H)] - \frac{\mu_2 s_2}{\mu_1 s_1}\right]$$

Roots $1 - \tan s_1 H \tan s_1 h = 0$ imply that

$$\text{(A-4)} \qquad s_1(h + H) = \pi/2, 3\pi/2, \ldots$$

which is inconsistent with the restriction that the nature of the period equation places upon this parameter. From Figure 3 it is evident that for a finite layer thickness $s_1(h + H)$ must be less than $\frac{n\pi}{2}$, $n = 1,2 \ldots$ for $\nu = \nu_n$ (period equation root), $n = 1,2,\ldots$, respectively. Roots $K = \frac{\omega}{c'}$ of the period equation

$$\text{(A-5)} \qquad \tan\left[s_1(h+H)\right] - \frac{\mu_2 s_2}{\mu_1 s_1} = 0$$

for the thicker layer have been assumed to lie on the edge of the analytic strip. Therefore $\Sigma(\nu)$ has no zeros in the strip.

In order to insure the convergence of the integrals (A-2), $\lim_{|\rho| \to \infty} q(\rho)$ must be zero. For the case being considered, this requirement takes the form $\lim_{|\nu| \to \infty} \Sigma(\nu) = +1$. From (60), with s_1, s_2 behaving as $i\nu$, ν respectively, as $|\nu| \to \infty$, it can be shown that

$$\text{(A-6)} \qquad \Sigma(\nu)\Big|_{|\nu|\to\infty} \approx \frac{2}{\nu}\Big|_{|\nu|\to\infty}$$

as long as $s_1 H$ is not equal to zero.

By virtue of (A-6), the function q cannot be the logarithm of $\Sigma(\nu)$ alone, but factors can be introduced to develop a function that does satisfy the necessary limit condition. Consider the function

$$\text{(A-7)} \qquad P(\nu) = \frac{1}{2}\sqrt{\nu^2 + |k_{\beta_2}|^2 \sin^2\epsilon}\ \Sigma(\nu).$$

Obviously, the term $\frac{1}{2}\sqrt{\nu^2 + |k_{\beta_2}|^2 \sin^2\epsilon}$ serves a two-fold purpose; it cancels the limiting $1/\nu$ dependence of $\Sigma(\nu)$ without introducing singularities in the strip $|\mathrm{Im}\nu| < |k_{\beta_2}| \sin\epsilon$ and brings the magnitude of $P(\nu)$ to unity as $|\nu| \to \infty$. Therefore, the method can be applied to $\ln P(\nu)$ as follows:

$$\text{(A-8)} \qquad q(\nu) = \ln P(\nu) = q^-(\nu) - q^+(\nu)$$

$$\text{(A-9)} \qquad q^+(\nu) = \frac{1}{2\pi i}\int_{-\infty - ia}^{\infty - ia} \frac{\ln P(\rho)}{\rho - \nu}\, d\nu \qquad 0 < a < |k_{\beta_2}| \sin\epsilon$$

$$(A\text{-}10) \qquad q^-(\nu) = \frac{1}{2\pi i} \int_{-\infty + ia}^{\infty + ia} \frac{\ell n\, P(\rho)}{\rho - \nu}\, d\rho \qquad 0 < a < |k_{\beta_2}| \sin \epsilon$$

so that

$$(A\text{-}11) \qquad P(\nu) = e^{q^-(\nu) - q^+(\nu)} = \frac{1}{2} \sqrt{\nu^2 + |k_{\beta_2}|^2 \sin^2 \epsilon}\; \Sigma(\nu)$$

or

$$(A\text{-}12) \qquad \Sigma(\nu) = \frac{2}{\sqrt{\nu^2 + |k_{\beta_2}|^2 \sin^2 \epsilon}}\, e^{q^-(\nu) - q^+(\nu)}$$

By (61), (A-9), (A-10), and (A-12),

$$(A\text{-}13) \qquad \sigma^+(\nu) = \frac{2}{\sqrt{\nu + i|k_{\beta_2}| \sin \epsilon}} \exp\left\{ \frac{-1}{2\pi i} \int_{-\infty - ia}^{\infty - ia} \frac{\ell n\, P(\rho)}{\rho - \nu}\, d\rho \right\}$$

$$(A\text{-}14) \qquad \sigma^-(\nu) = \sqrt{\nu - i|k_{\beta_2}| \sin \epsilon} \exp\left\{ \frac{-1}{2\pi i} \int_{-\infty + ia}^{\infty + ia} \frac{\ell n\, P(\rho)}{\rho - \nu}\, d\rho \right\}$$

The functions $\sigma^+(\nu)$ and $\sigma^-(\nu)$ are regular and zeroless in the half planes $\mathrm{Im}\nu > -a$ and $\mathrm{Im}\nu < a$ respectively, and it can be shown that $|\sigma^+(\nu)|$ and $|\sigma^-(\nu)|$ lie between positive bounds as $|\nu|$ becomes large in their respective half planes of regularity. Thus $\sigma^+(\nu)$ and $\sigma^-(\nu)$ satisfy the properties listed in (61).

A calculation of the exponentials in (A-13) and (A-14) is unlikely due to the complexity of the integrals. In order to benefit from the factorization, the integrals in (A-13) and (A-14) must be reduced to forms that are solvable, either analytically or numerically.

A formal manipulation of $\sigma^-(\nu)$ including a substitution $\rho = -\rho'$

and a reversal of limits of integration yields:

$$\text{(A-15)} \qquad \sigma^-(-\nu) = 2\sqrt{\frac{-\nu - i|k_{\beta_2}|\sin\epsilon}{\nu + i|k_{\beta_2}|\sin\epsilon}} \cdot \frac{1}{\sigma^+(\nu)}$$

In the expressions (75), (76), and (79), all terms are real except $\sigma^+(K)$, $\sigma^+(\alpha)$, and $\sqrt{\frac{-\alpha - i|k_{\beta_2}|\sin\epsilon}{\alpha + i|k_{\beta_2}|\sin\epsilon}}$. Therefore, to obtain the magnitude of the transmission and reflection coefficients, one needs to take the absolute value of only these factors, all others presenting no difficulty. It is obvious that the magnitude of the above radical is unity. As for $|\sigma^+(K)|$, the analysis is as follows: By (A-13),

$$\text{(A-16)} \qquad |\sigma^+(K)| = \frac{2}{\left|\sqrt{K + i|k_{\beta_2}|\sin\epsilon}\right|} \left| \exp\left\{\frac{-1}{2\pi i}\int_{-\infty - ia}^{\infty - ia} \frac{\ell n\, P(\rho)}{\rho - K}\, d\rho\right\}\right|$$

$$= \frac{2}{\left|\sqrt{K + i|k_{\beta_2}|\sin\epsilon}\right|} \exp\left\{\mathrm{Im}\left[\frac{-1}{2\pi}\int_{-\infty - ia}^{\infty - ia} \frac{\ell n\, P(\rho)}{\rho - K}\, d\rho\right]\right\}.$$

Letting the width of the analytic strip approach zero ($\epsilon \to 0$) such that

$$\text{(A-17)} \qquad \sqrt{K + i|k_{\beta_2}|\sin\epsilon} \to \sqrt{K}, \quad P(\nu) \to \frac{1}{2}\nu\,\Sigma(\nu)$$

and the contour of integration becomes the real axis with suitable indentations around $\rho = \pm K, \pm\alpha$, and $\pm k_{\beta_2}$, and noting that $P(\rho)$ is even yields:

$$\text{(A-18)} \qquad |\sigma^+(K)| = \frac{2}{\sqrt{K}} \exp\left\{\mathrm{Im}\left[\frac{-K}{\pi}\int_0^{\infty} \frac{\ell n[\frac{1}{2}\rho\,\Sigma(\rho)]}{\rho^2 - K^2}\, d\rho\right]\right\}$$

An inspection of (60) shows that, for $\rho > k_{\beta_2}$, ρ real, $\Sigma(\rho)$ is real, so that the integration in the region $k_{\beta_2} < \rho < \infty$ produces no imaginary part. For $0 \le \rho \le k_{\beta_2}$, $\Sigma(\rho)$ is complex, with

$$\text{(A-19)}\quad \mathrm{Re}[\Sigma(\rho)] = -\frac{\cot s_1 H}{s_1} + \frac{\frac{\mu_2}{\mu_1}\frac{\bar{s}_2}{s_1}\sin s_1 h\ \mathrm{Im}[\delta(\rho)] - \cos s_1 h\ \mathrm{Re}[\delta(\rho)]}{\left\{\mathrm{Re}[\delta(\rho)]\right\}^2 + \left\{\mathrm{Im}[\delta(\rho)]\right\}^2}$$

and

$$\text{(A-20)}\quad \mathrm{Im}[\Sigma(\rho)] = \frac{\frac{\mu_2}{\mu_1}\frac{\bar{s}_2}{s_1}\sin s_1 h\ \mathrm{Re}[\delta(\rho)] + \cos s_1 h\ \mathrm{Im}[\delta(\rho)]}{\left\{\mathrm{Re}[\delta(\rho)]\right\}^2 + \left\{\mathrm{Im}[\delta(\rho)]\right\}^2}$$

where

$$\mathrm{Re}[\delta(\rho)] = s_1 \sin s_1 h\ , \qquad \mathrm{Im}[\delta(\rho)] = \frac{\mu_2}{\mu_1}\bar{s}_2 \cos s_1 h$$

(A-21)

$$s_1 = s_1(\rho) = \sqrt{k_{\beta_1}^2 - \rho^2}\ , \qquad s_2 = s_2(\rho) = -i\sqrt{k_{\beta_2}^2 - \rho^2} = -i\bar{s}_2$$

Expressing $\ell n[\frac{1}{2}\rho\Sigma(\rho)]$ as $\ell n[|\frac{1}{2}\rho\Sigma(\rho)|] + i\Phi(\rho)$, where

$$\text{(A-22)}\qquad \Phi = \tan^{-1}\left\{\frac{\mathrm{Im}[\Sigma(\rho)]}{\mathrm{Re}[\Sigma(\rho)]}\right\}$$

(A-18) can be written

$$\text{(A-23)}\qquad |\sigma^+(K)| = \frac{2}{\sqrt{K}}\exp\left\{-\frac{K}{\pi}\int_0^{k_{\beta_2}}\frac{\Phi(\rho)}{\rho^2 - K^2}\,d\rho\right\}$$

This form of the factor is still generally unsolvable, for the values of k_{β_2} and K are usually unknowns, and, even if they were available, the complexity of the integrand makes any attempt at formal integration futile.

It is possible to make a change of variable that surmounts these difficulties. Let $\rho = k_{\beta_2}\eta$ which results in

$$(A\text{-}24) \qquad |\sigma^{+}(K)| = \frac{2}{\sqrt{K}} \exp\left\{\frac{1}{\pi}\frac{k_{\beta_2}}{K}\int_0^1 \frac{\Phi(\eta)}{1-\frac{k_{\beta_2}}{K}\eta^2}\,d\eta\right.$$

where

$$(A\text{-}25) \qquad s_1 = s_1(\eta) = k_{\beta_2}\sqrt{\left(\frac{\beta_2}{\beta_1}\right)-\eta^2}\,, \quad \bar{s}_2 = \bar{s}_2(\eta) = k_{\beta_2}\sqrt{1-\eta^2}$$

The ratios of propagation constants can be obtained from the period equation and knowledge of the value of the ratio of the shear wave velocities β_1 and β_2, making calculation of the real and imaginary parts of $\Sigma(\eta)$ possible. Although analytical integration is still fairly impossible, (A-24) is of a form such that $|\sigma^{+}(K)|$ can be evaluated numerically.

By a similar procedure the factor $|\sigma^{+}(\alpha)|$ is represented by an expression identical to (A-24), except that α replaces K. Thus the expressions (75),(76), and (79) for the transmission and reflection coefficients can be programmed on a digital computer, the integration in (A-24) being approximated numerically. The end results of these calculations are in principle the coefficients desired.

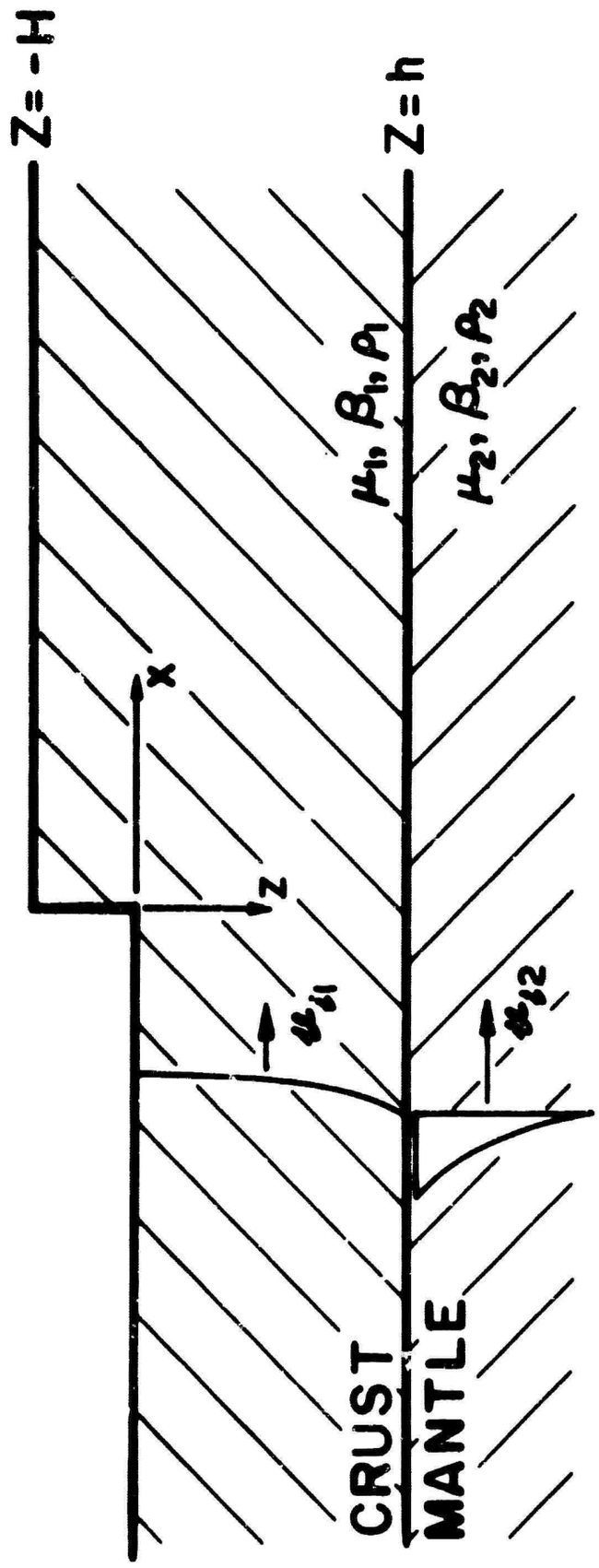

FIGURE 1 GEOMETRY OF THE PROBLEM

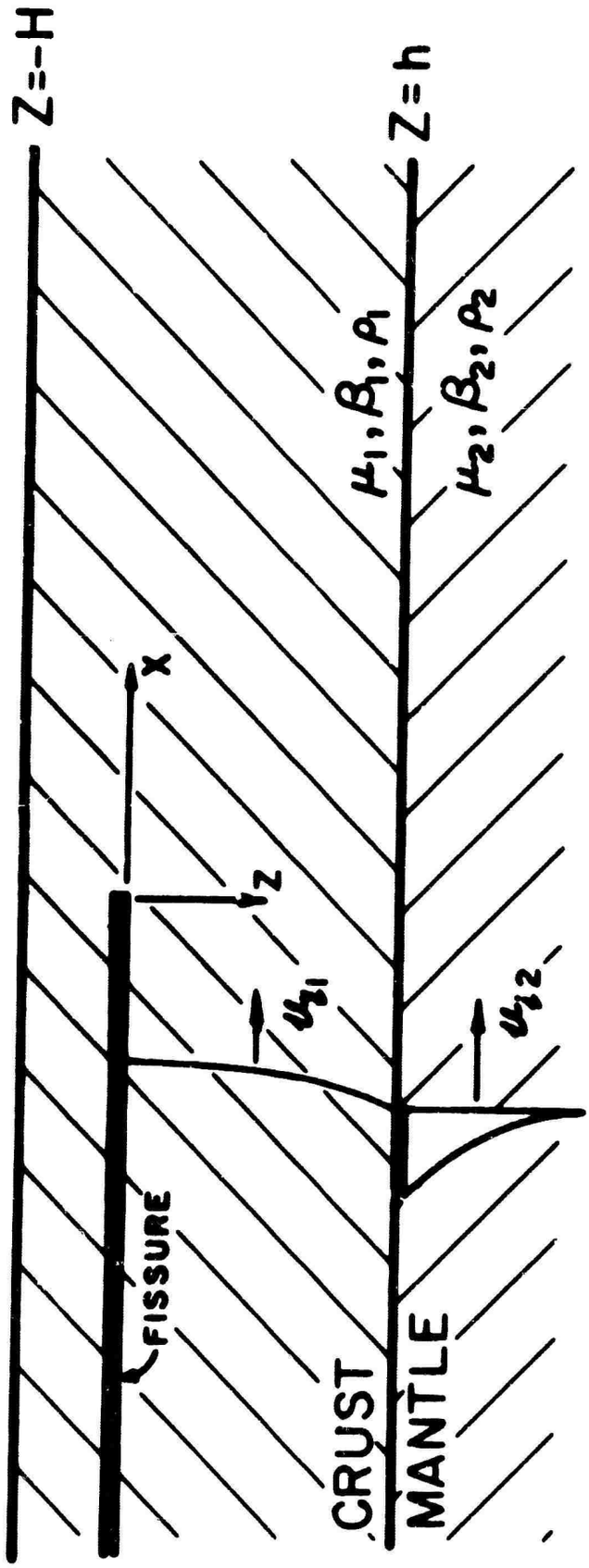

FIGURE 2 MODIFIED GEOMETRY OF THE PROBLEM

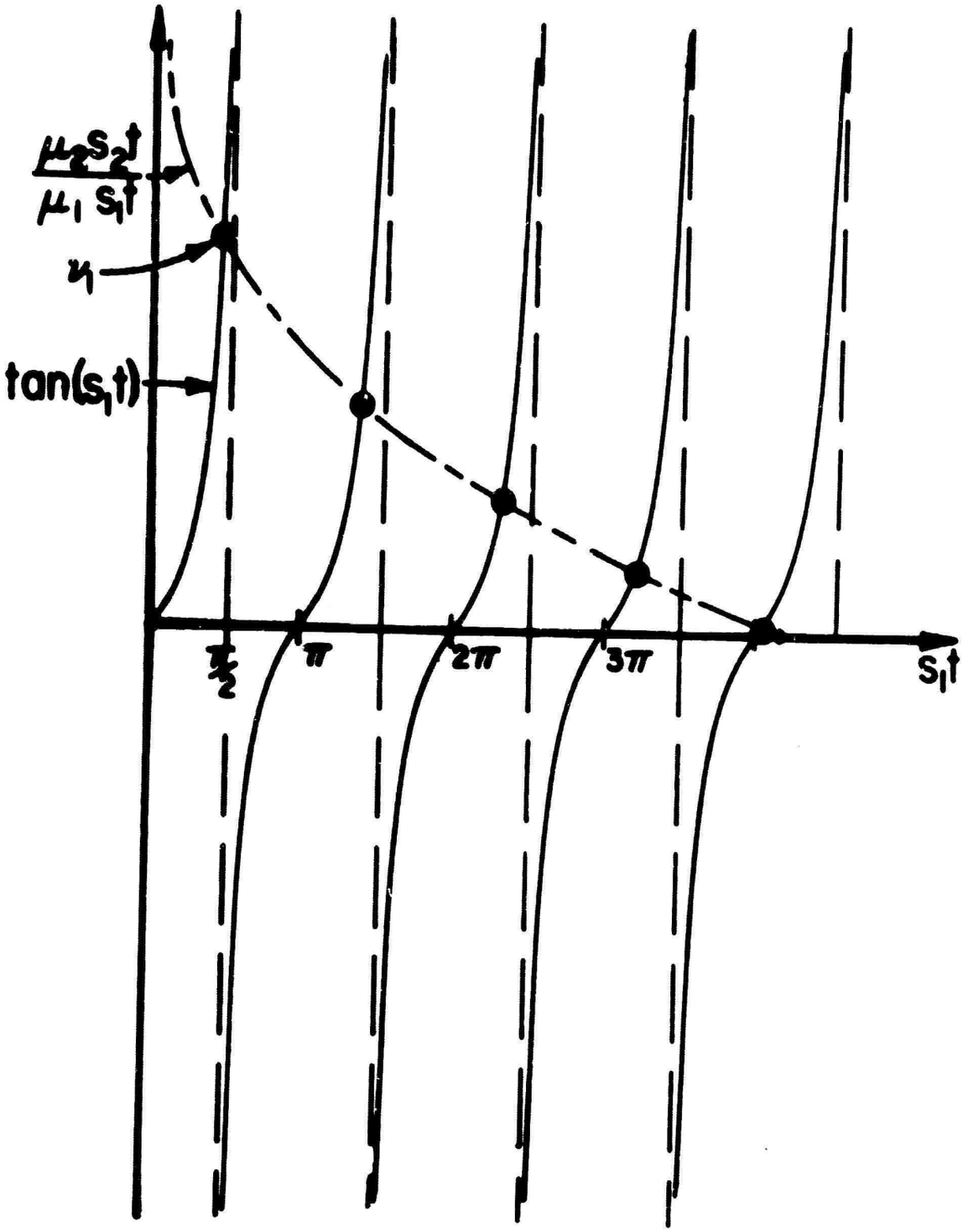

FIGURE 3 ROOTS OF THE PERIOD EQUATION (24)

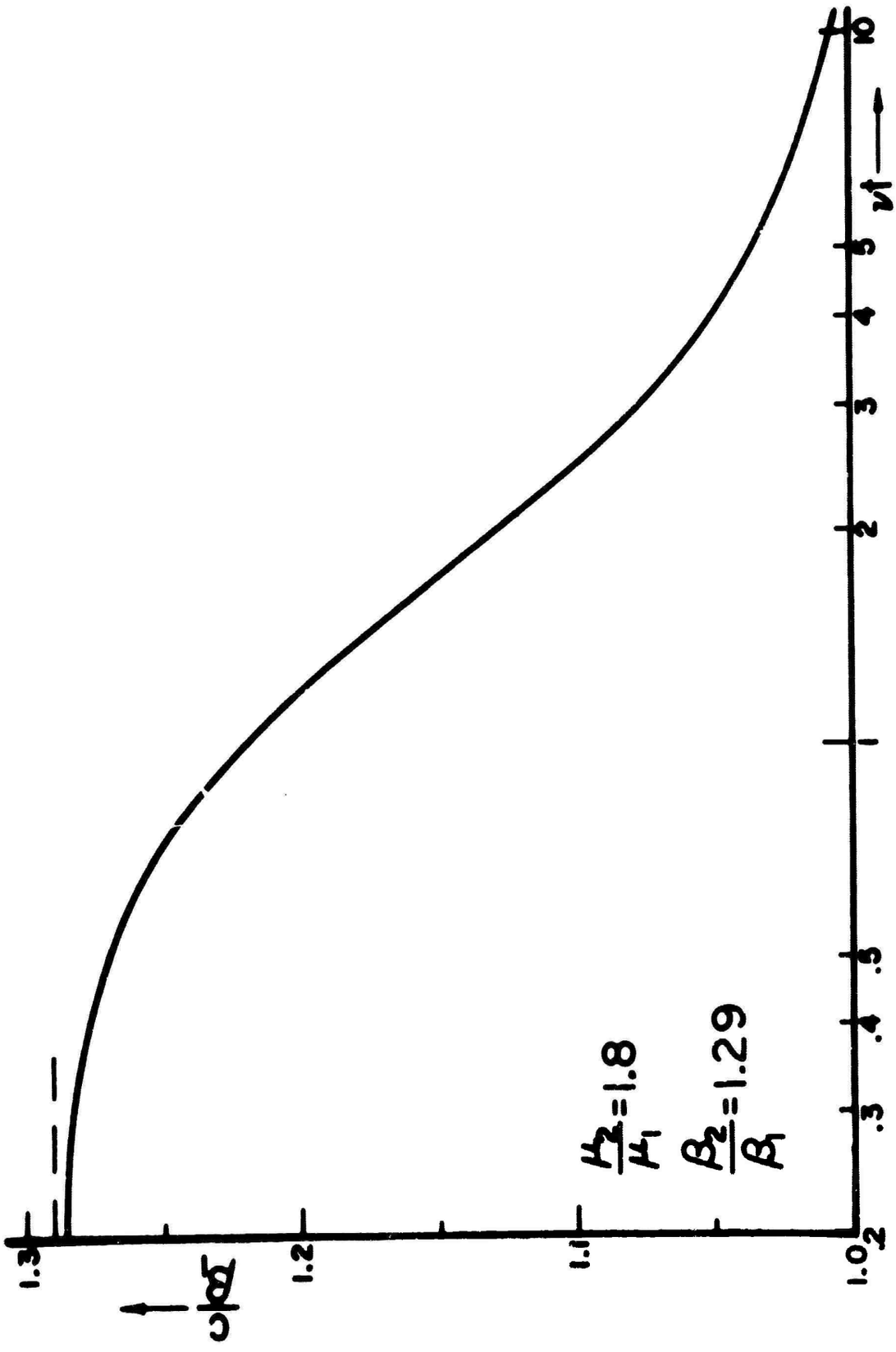

FIGURE 4 FUNDAMENTAL LOVE WAVE PHASE VELOCITY

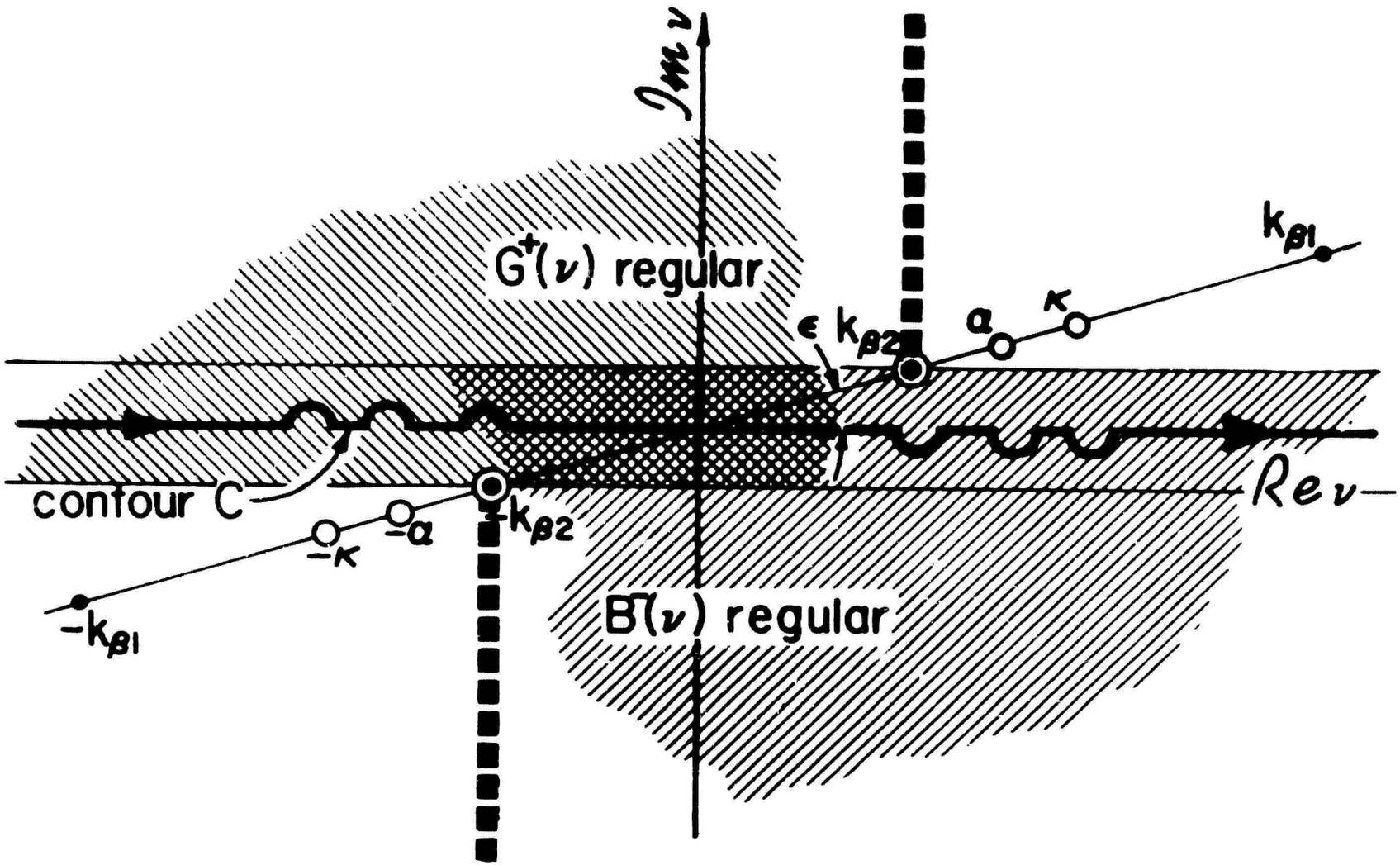

FIGURE 5 THE COMPLEX ν - PLANE

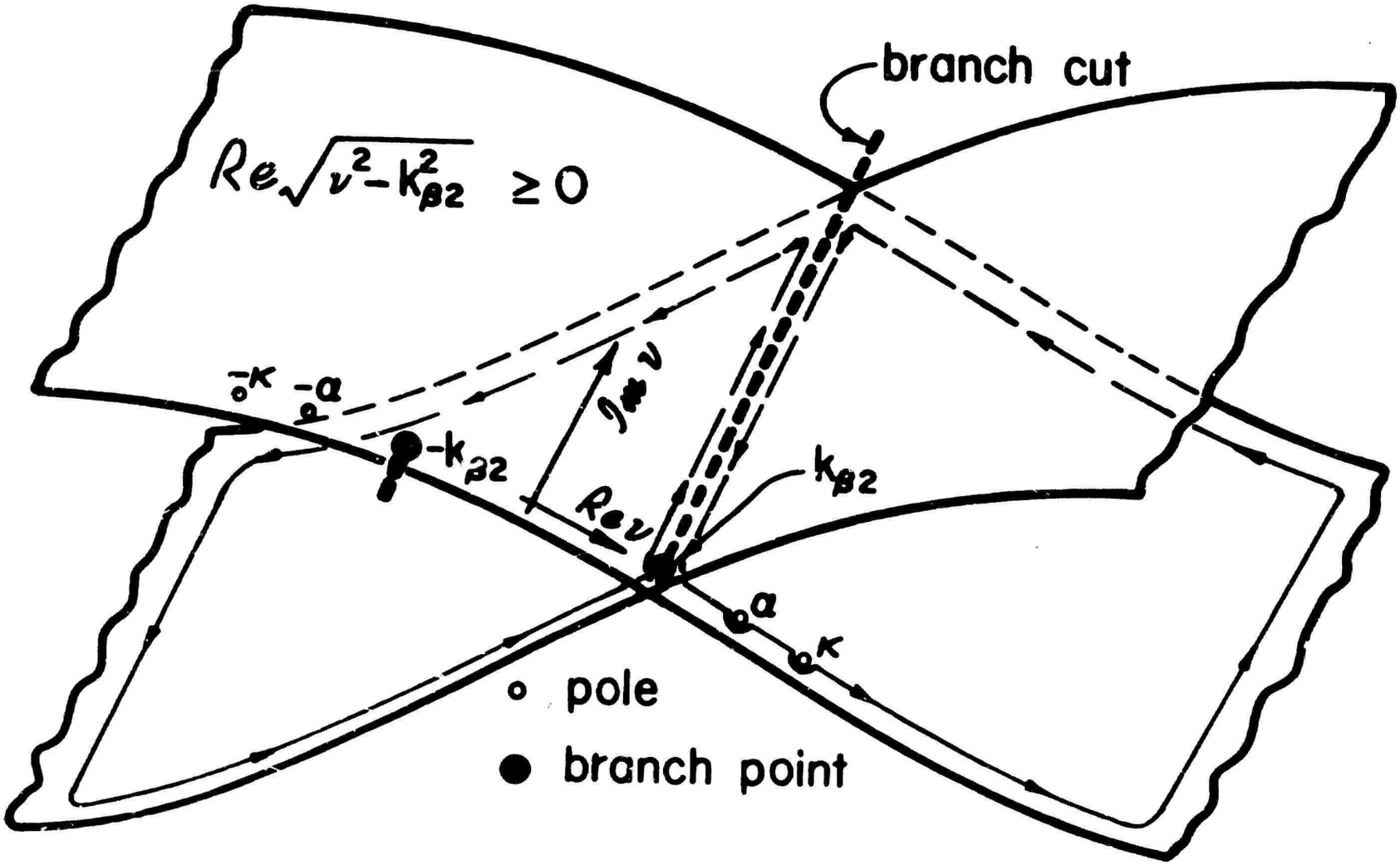

FIGURE 6 ν-PLANE CONTOUR FOR TRANSMITTED FIELDS

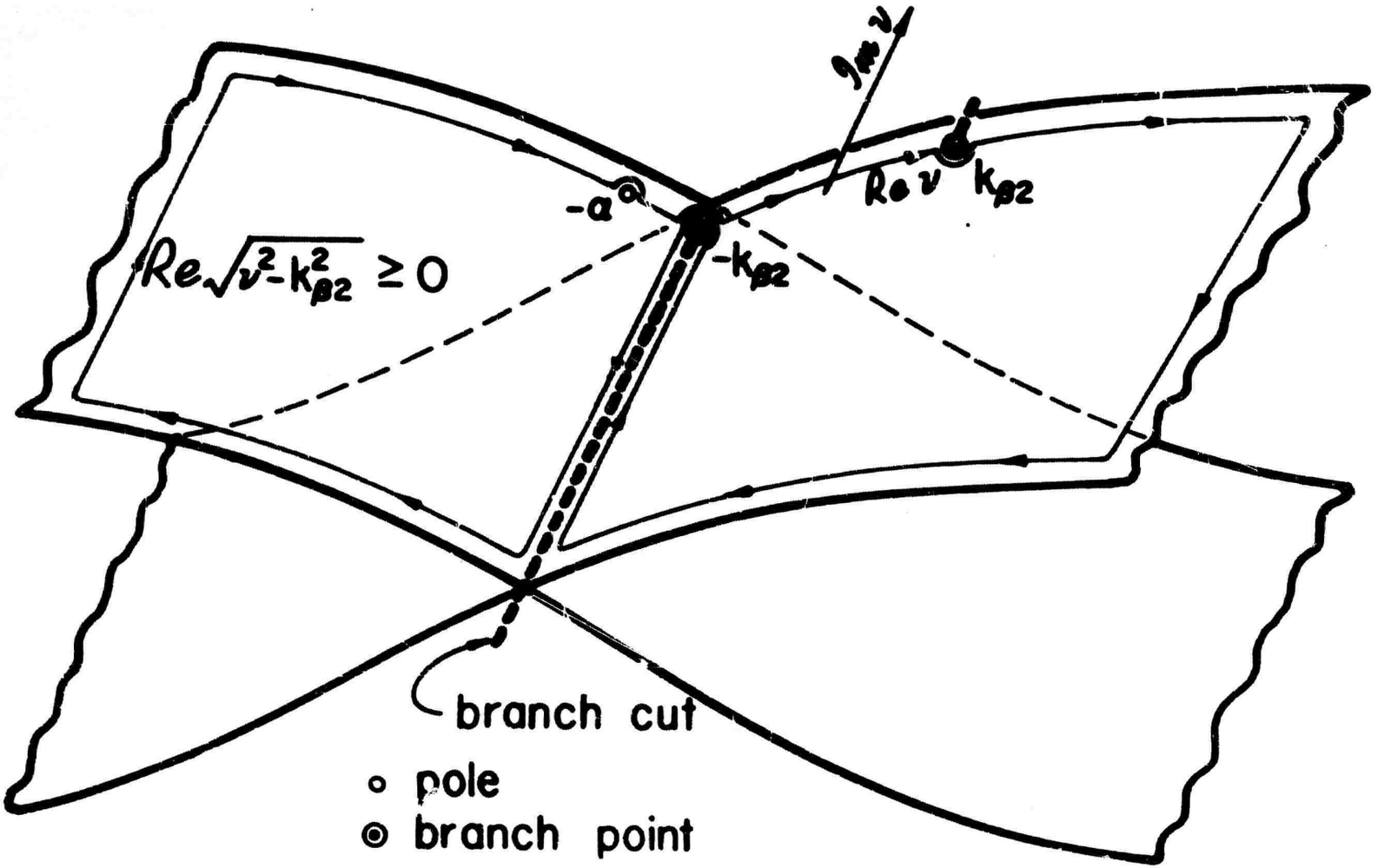

FIGURE 7 ν-PLANE CONTOUR FOR REFLECTED FIELDS

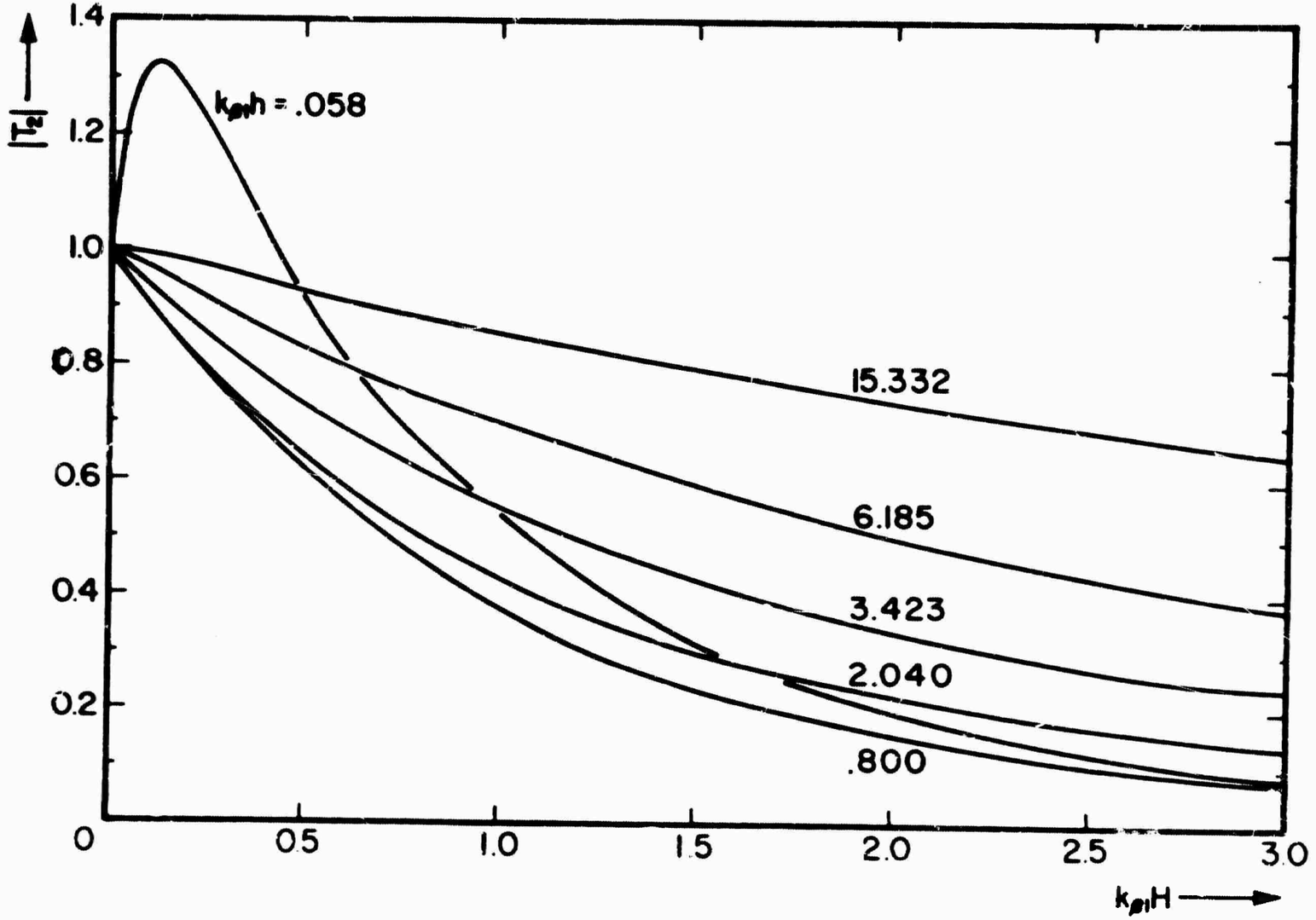

FIGURE 8 THE TRANSMISSION COEFFICIENT $|T_2|$

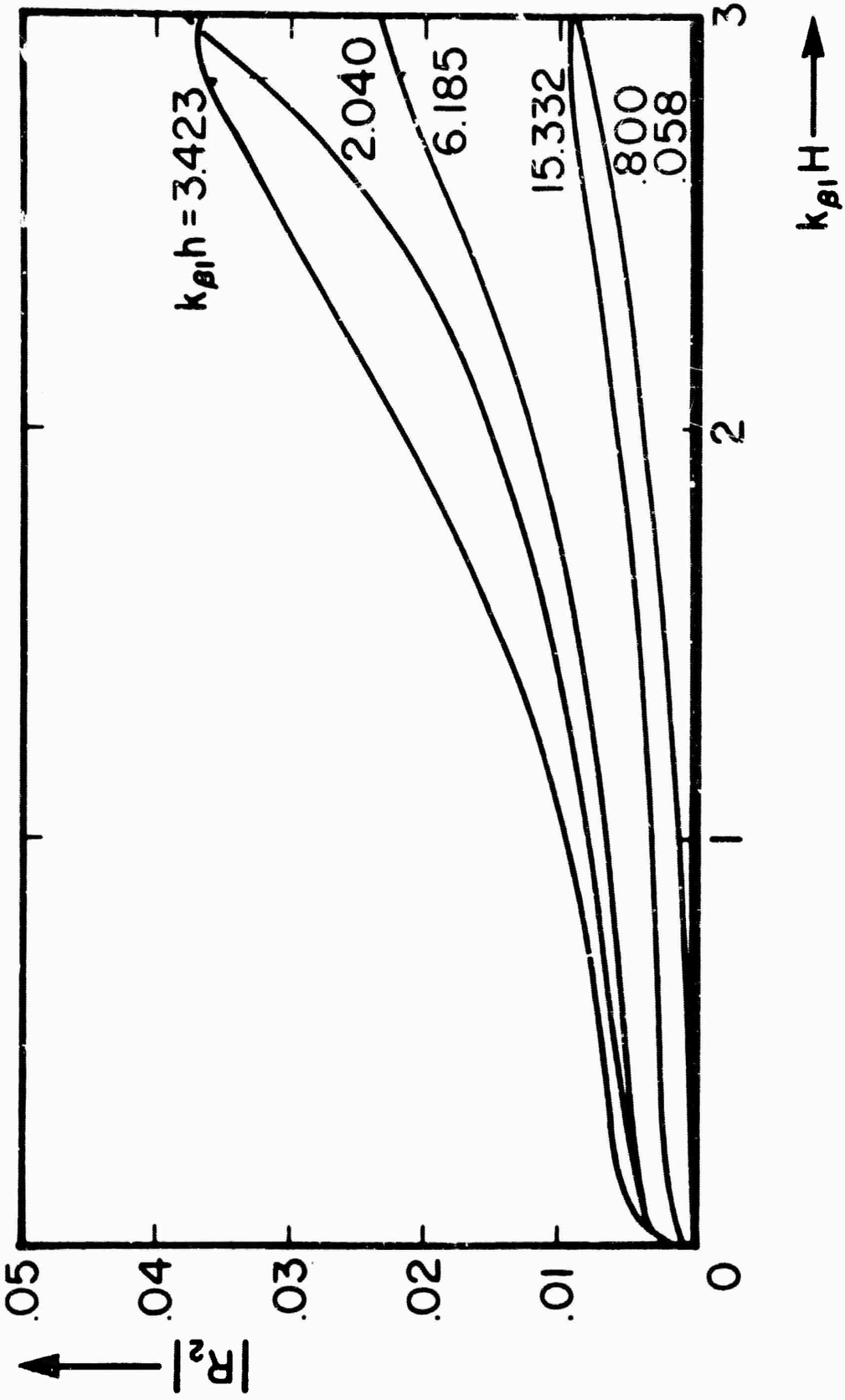

FIGURE 9 THE REFLECTION COEFFICIENT $|R_2|$

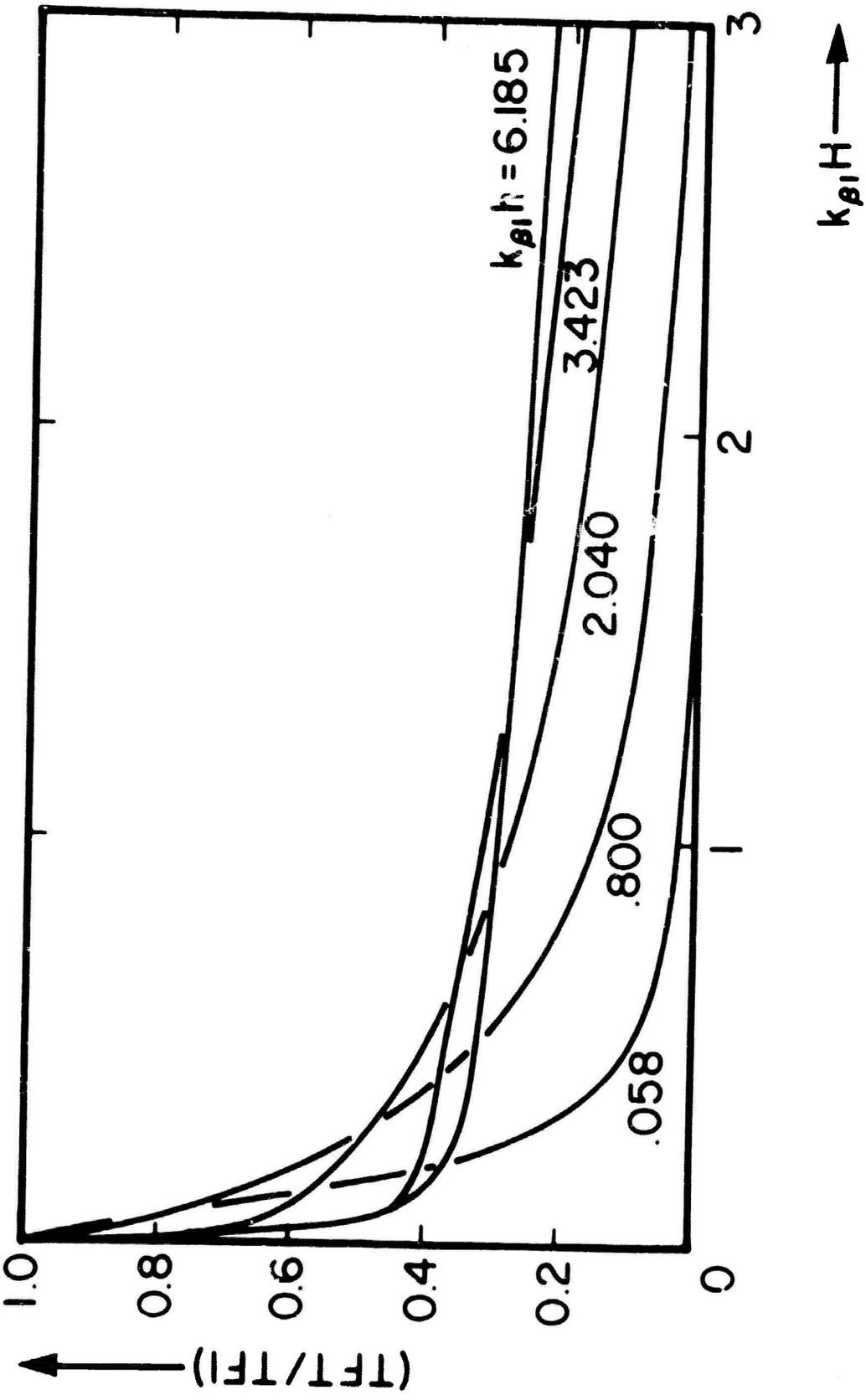

FIGURE 10 PERCENTAGE OF INCIDENT ENERGY IN THE TRANSMITTED LOVE WAVE

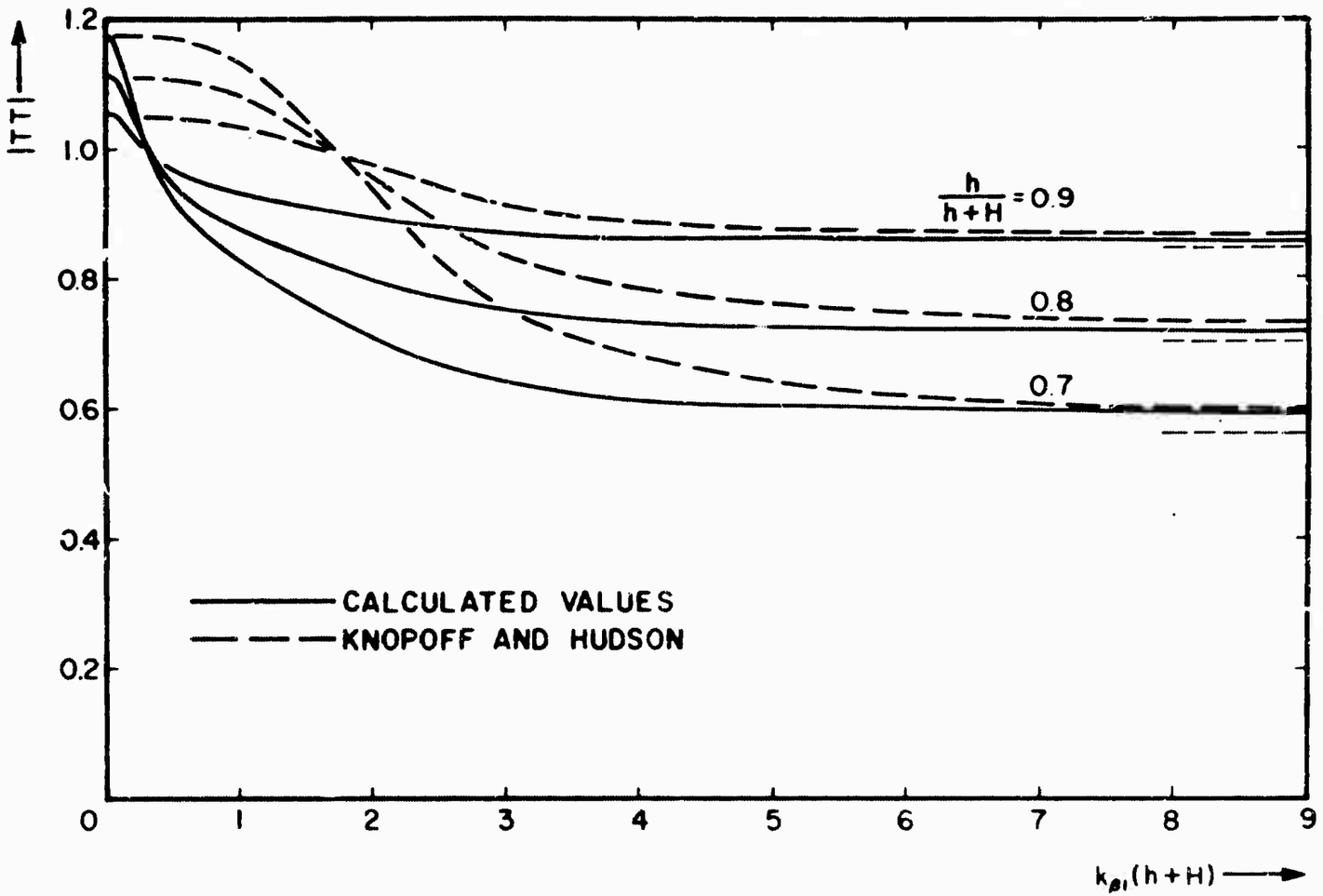

FIGURE 11 COMPARISON OF |TT| WITH THE RESULTS OF KNOPOFF AND HUDSON

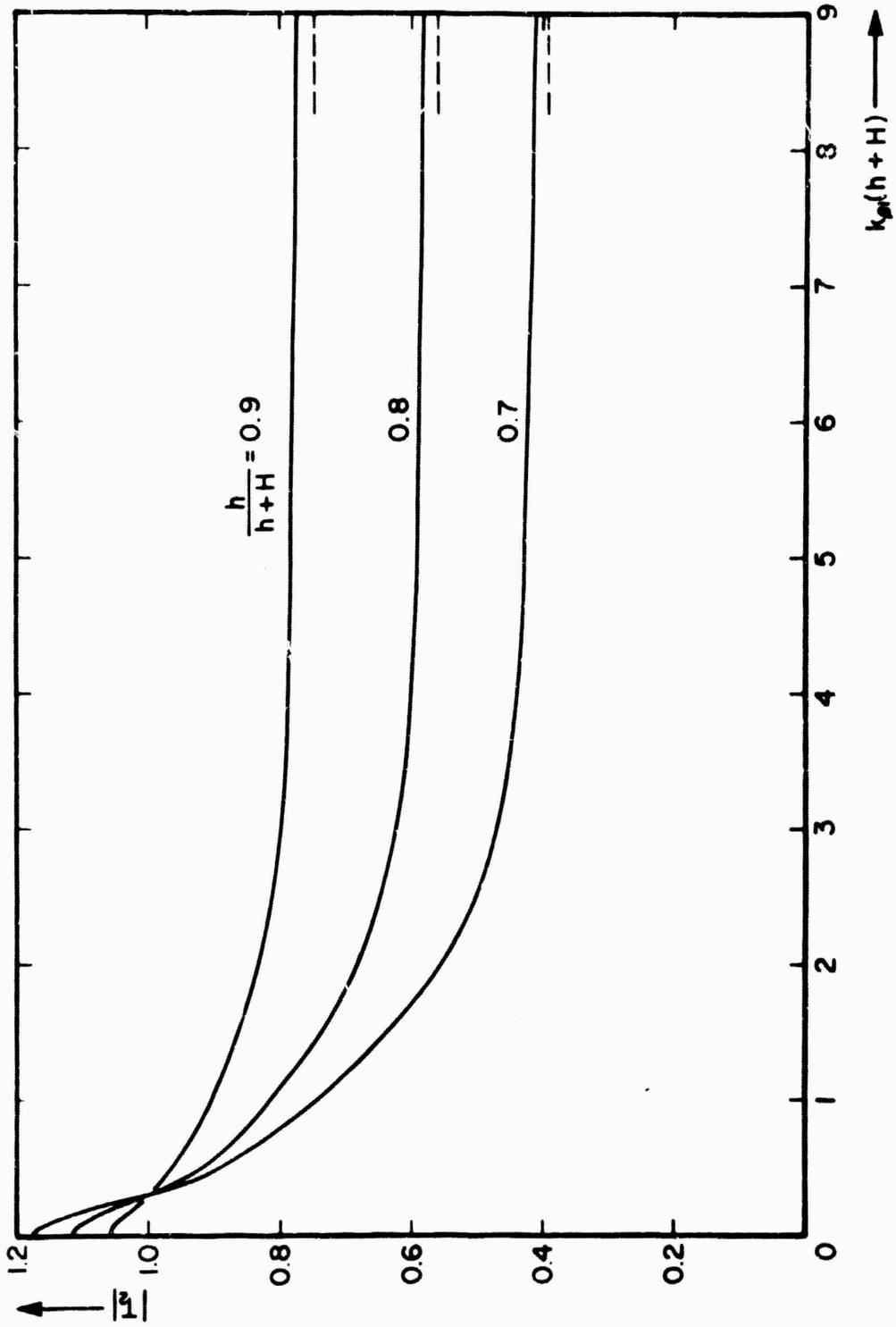

FIGURE 12 THE COEFFICIENT $|T_2|$ VIA THE METHOD OF KNOPOFF AND HUDSON

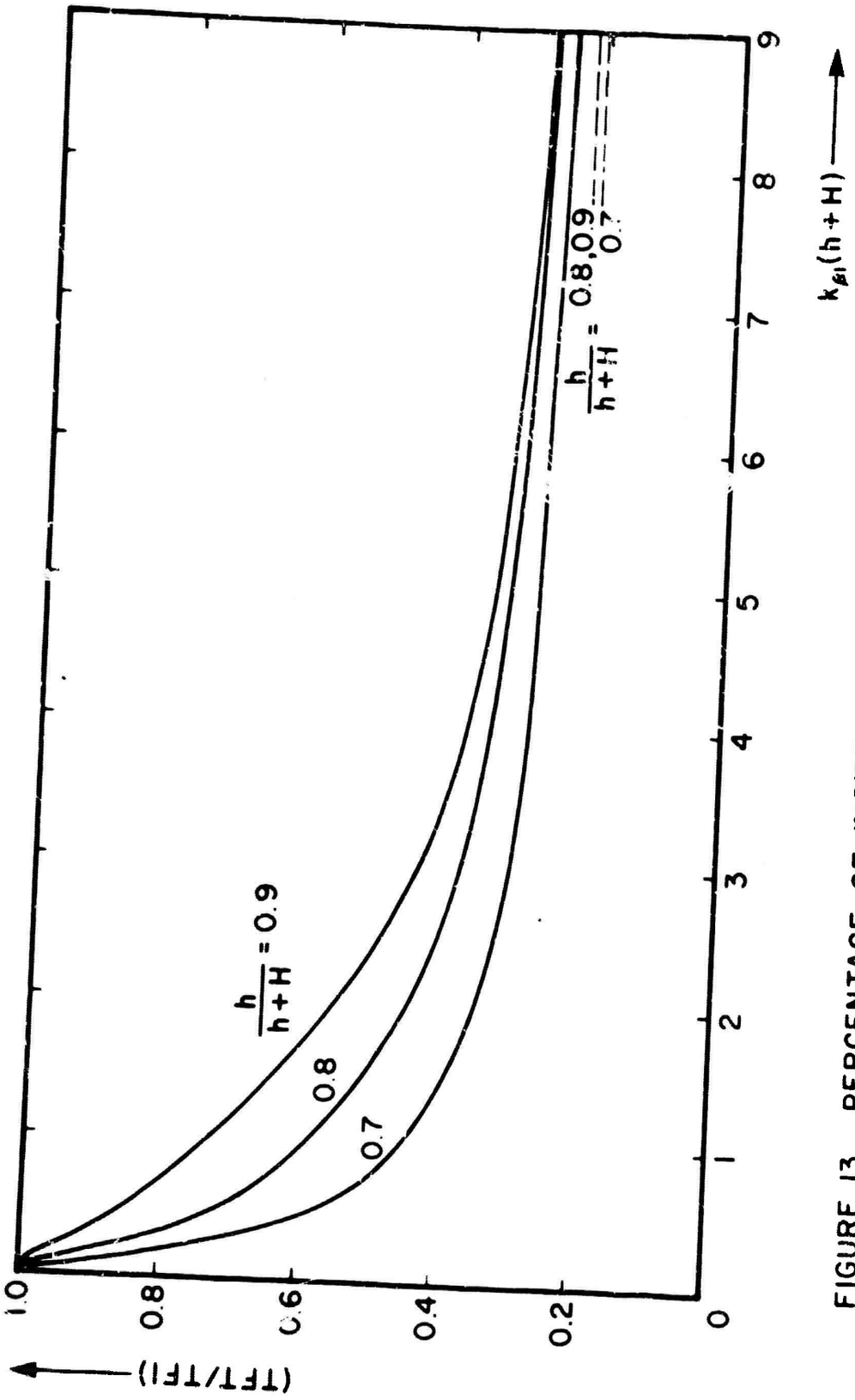

FIGURE 13 PERCENTAGE OF INCIDENT ENERGY IN THE TRANSMITTED LOVE WAVE VIA THE METHOD OF KNOPOFF AND HUDSON

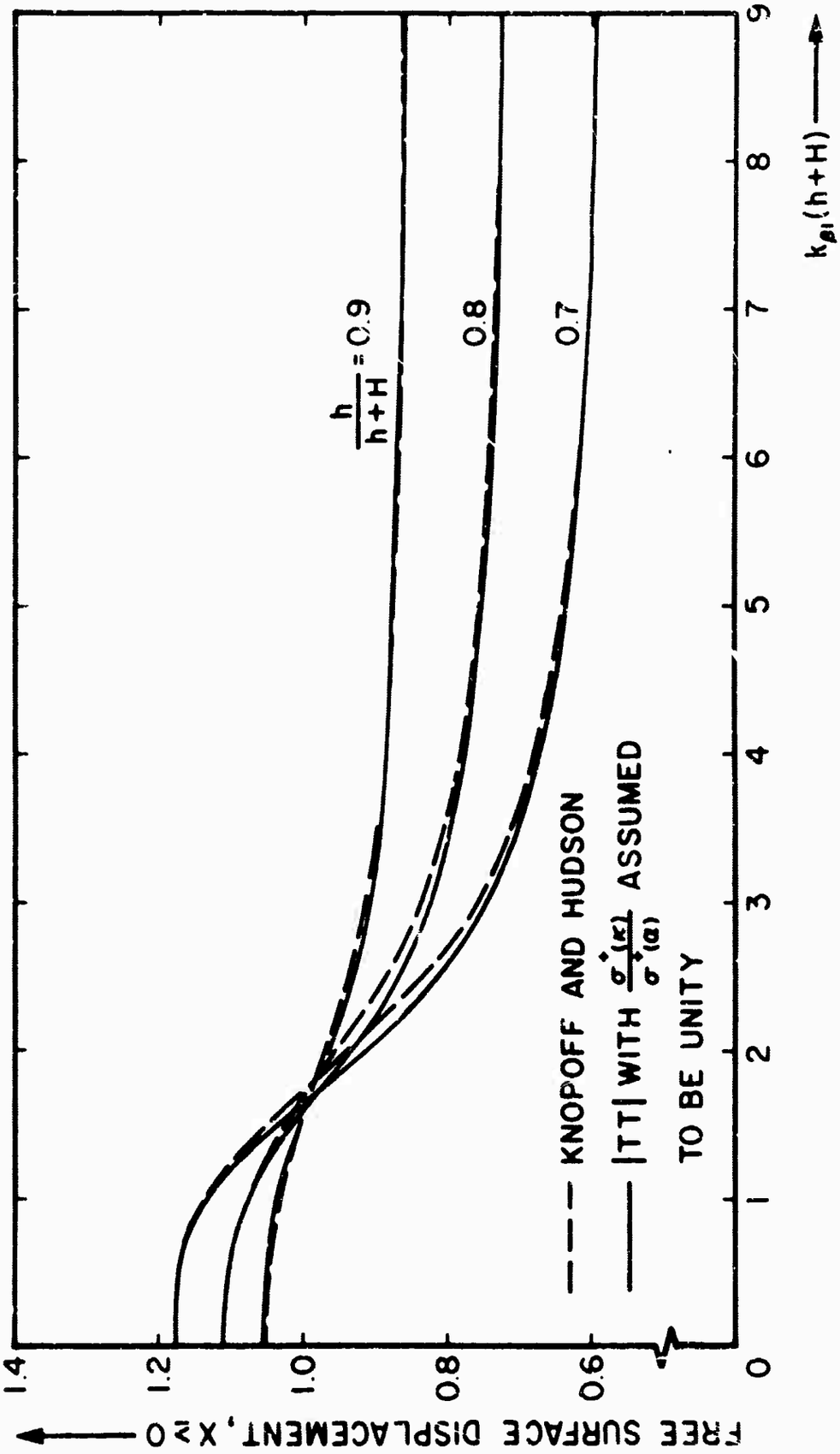

FIGURE 14 COMPARISON OF APPROXIMATE |TT| WITH THE RESULTS OF KNOPOFF AND HUDSON